University of
South-Eastern Norway

www.usn.no

FMH606 Master's Thesis 2022
Electrical Power Engineering

# Sensitivity analysis of low voltage distribution grid in rural areas with high penetration of PV systems

Anders Berger

Faculty of Technology, Natural Sciences and Maritime Sciences
Campus Porsgrunn

University of South-Eastern Norway
www.usn.no

**Course:** FMH606 Master's Thesis 2022
**Title:** *Sensitivity analysis of low voltage distribution grid in rural areas with high penetration of PV systems*
**Pages:** *96*
**Keywords:** *Distribution grid, PV systems, voltage quality, voltage rise, THD, harmonic flow analysis, load flow analysis, PowerFactory, sensitivity analysis*

**Student:** *Anders Berger*
**Supervisor:** *Thomas Øyvang and Gunne John Hegglid*
**External partner:** *Lede AS*

**Summary:**
PV systems are one of the most increasing renewable energy sources globally. In Norway, PV systems increase in amount and size, and it is becoming more critical to have solid knowledge in incorporating them into older grid systems.

This master thesis investigates the impact of PV systems on the low voltage grid and the impact on the power quality terms. The objective is to evaluate the PV capacity regarding voltage limits, THD, and thermal overload to describe a grid investment threshold.

The utility company Lede AS provides this thesis with necessary data for consumer measurements and network information system. Four study cases of existing grid systems from rural areas with few customers are modeled using PowerFactory. These grid systems represent the most challenging area for the utility company to incorporate PV systems.

In order to understand the PV capacity in these grids, the four study cases evaluate four different scenarios. The first two scenarios will investigate the PV capacity in specific scenarios, and the last two will investigate the impact on PV capacity by reinforcing the grid. Customers close to the substation and generally farms have a high PV capacity. Changing the transformer has little effect in improving the PV capacity of the circuit. Changing the feeding lines to cables with higher capacity have a better effect on improving the PV capacity in the circuits.

The simulation results show that the parameter voltage variation most often limits the PV capacity in a rural grid area with high PV penetration. The thesis proposes an equation with a consideration method for the DSO to decide if the grid needs investment regarding integrating new prosumers into the grid. In Lede AS' grid area, 746 of 7172 substation circuits have a higher risk of needing an upgrade because of PV systems.

# Preface

This thesis concludes my last work through the master's degree program in Electrical Power Engineering at the University of South-Eastern Norway (USN). I am thankful for the opportunity from my employer, Lede AS to be able to study Electrical Power Engineering and in particular get to immerse myself in the topic of voltage quality.

I want to thank my supervisor Thomas Øyvang and co-supervisor Gunne J. Hegglid, for good guidance, critical view and feedback throughout the thesis. Thanks to Lede AS, for supporting with data and making this thesis possible. From Lede I would like to thank Marte Neslow and Ivan Schytte for their support and consulting.

Porsgrunn, 16th May 2022

Anders Berger

# Contents

# List of Figures

# List of Tables

# Nomenclature

| Symbol | Explanation |
|---|---|
| AC | Alternating Current |
| AC-DC | (Alternating Current to Direct Current) |
| AMS | Advanced Metering- and Control-system |
| DC | Direct Current |
| DSO | Distributed System Operator |
| EMC | Electromagnetic compatibility |
| GDPR | General data protection regulation |
| IEA | International Energy Agency |
| IGBT | Insulated-gate bipolar transistor |
| MOSFET | Metal Oxide Silicon Field-Effect Transistor |
| NIS | Network Information System |
| NVE | The Norwegian Water Resources and Energy Directorate |
| NVE-RME | The Norwegian Energy Regulatory Authority |
| OLTC | On-Load Tap-Changer Control |
| PCC | Point of common coupling |
| PR | Performance ratio |
| PQA | Power Quality Analysis |
| PV | Photovoltaic |
| PWM | Pulse width modulation |
| REN | Company for Norwegian collaboration between DSO's |
| RMS | Root-Mean-Square |
| TSO | Transmission System Operator |
| UN | United Nations |
| USN | University of South-Eastern Norway |

# Subscripts

| **Symbol** | **Explanation** | **Unit symbol** |
|---|---|---|
| A | Surface area | $m^2$ |
| $\alpha$ | Temperature coefficient | $1/K$ |
| $C_p$ | Specific heat capacity | $J/(kg \cdot K)$ |
| E | Energy | $Wh$ or $J$ |
| f | Frequency | $Hz$ |
| $\varepsilon$ | Emissivity | - - |
| h | Convective heat transfer coefficient | $Watt/(m^2K)$ |
| I | Current | $A$ |
| $I_F$ | Effective voltage of fundamental | $A$ |
| $I_H$ | Effective Voltage of all the harmonic | $A$ |
| l | Length | $m$ |
| m | Mass | $kg$ |
| P | Active power | $W_p$ |
| $\phi$ | Angle | $^\circ$ |
| - | Base unit | $pu$ |
| Q | Reactive power | $var$ |
| $Q_E$ | Quantity of heat | $J$ |
| R | Resistance | $\Omega$ |
| S | Apparent power | $VA$ |
| T | Temperature | $K$ or $^\circ C$ |
| t | Time | $s$ |
| THD | Total Harmonic Distortion | $\%$ |
| U | Voltage | $V$ |
| $U_F$ | Effective voltage of fundamental | $V$ |
| $U_H$ | Effective Voltage of all the harmonic | $V$ |
| X | Reactance | $\Omega$ |
| Z | Impedance | $\Omega$ |

# 1 Introduction

To respond to climate challenges, the Paris Agreement is a legally binding, international UN (United Nations) treaty that aims to keep global warming well below 2°C [1]. One action is to reduce emissions from fossil energy sources by replacing them with renewable energy sources such as wind, solar, and hydropower. The IEA (International Energy Agency) reported that in 2020 the total generated electricity from solar PV (Photovoltaic) increased globally by 156 $TWh$ (23%) to a total production of 821 $TWh/year$. The cost of installing PV systems decrease, and it can soon be the lowest-cost option [2].

In Norway, the total yearly electricity generation with solar PV is 0,15 $TWh$. This is about one per mille of Norway's total electric production. The installed capacity at the end of 2021 was 205 $MW_p$. 186 $MW_p$ is grid-connected PV systems, and about 19 $MW_p$ is off-grid PV systems. Off-grid systems are typically found on cabins, lighthouses, and base stations for telephone towers have been used for the last 20-25 years, while grid-connected has had significant growth in the last 6-7 years. Now in 2022, over 90 % of PV systems are grid-connected in Norway [3].

There is an increasing trend of PV installations in Norway. These installations produce power to both meet the households' power consumption but also be able to deliver power to the grid side. Lede AS have experienced some customers struggling with voltage quality after installing PV systems. There is a need for more knowledge regarding PV systems' impact on the voltage quality of the grid. Satisfying voltage quality is critical for the end-user and the coordination at the grid side.

## 1.1 Background

According to Norwegian regulation, a DSO (Distributed System Operator) must calculate a contribution fee if a customer causes investment in the grid by; connecting to the grid, increasing his or her capacity, or increasing his or her quality [4]. Existing customers of the grid have the right to use their assigned PV capacity, to produce and deliver the same amount of power out to the grid as they are allowed to consume from the grid, without a contribution fee [5]. This means that the main supply fuse or overload protection limits the customers' production. If a customer wants to produce more than the main supply fuse allows, he or she would need to increase the capacity, resulting in a possible contribution fee from the DSO. The DSO is responsible for reinforcing the grid in the event of unsatisfying voltage quality. Historically, production units have not been commercial in the low voltage distribution grid. Therefore, the previous grid architects considered all customers only to consume electricity from the grid, and they built the existing grid for customers to be pure loads. In the last thirty years, small-scale hydropower plants have challenged the high voltage distribution grid. The challenge have been to integrate these production units into an existing high voltage distribution grid. In the previous 5-7 years, with decreasing costs combined with incentives for installing PV systems, the development in PV installations have increased and may challenge the existing low voltage distribution grid [6].

## 1.2 Motivation

The increasing number of prosumers causes the motivation of this project; to be proactive in understanding the potential problems in the grid before they happen. Moreover, to increase knowledge regarding grid planning to utilize the grid most efficiently.

The current grid is not built to sustain voltage rise. Many existing grid system needs evaluation for whether they can handle implementation of PV systems, or not. As newer circuits are stronger and better prepared to handle PV systems, this thesis focus on implementing PV systems in the existing low voltage grid.

## 1.3 Problem statement

The main goal of this project is to analyze the impact of high penetration of PV systems on the existing grid. The DSO, Lede AS provides the data. The data will be used in grid simulations and sensitivity analysis to determine the impact of PV systems on different grid parameters. Simulation results are used to find one or more thresholds parameters that triggers an investment in the grid caused by PV systems. The following sub-goals are:

- Find a general threshold that can determine when the grid needs investment to handle new PV installation for households in the grid.
- Map the development of PV installations.
- Investigate the future need for investments in Lede's grid to meet the growth of PV installations.
- Investigate different countermeasures that can handle the future requirements of the grid.

The word investment in this thesis is meant as assets invested in the grid to either reduce losses and disconnections from fault events, increase operation efficiency or maintain voltage quality despite changes in consumption or production.

This thesis will focus on substation circuits in rural areas with IT network. Industrial and urban areas will not be regarded. One-phase inverters and voltage imbalance have not been studied. The thesis disregards parts of voltage quality, such as flickering and rapid voltage changes. These parameters are considered less important for PV systems' impact on the grid than slow voltage variations, thermal load, and harmonic distortion. The impact on relays in distribution grid will not be simulated in this thesis.

## 1.4 Execution and structure of the thesis

Lillebo, Kirkeby and Holm from PQA have simulated and discussed the impact of PV systems on different types of grid systems [6]. This thesis will follow up on this report and look more into impact on existing rural grid systems in Norway. The project chooses four substation circuits that can represent typical circuits and uses DIgSILENT PowerFactory to create models of the circuits. The project collects necessary grid and consumption data to simulate different cases to understand better the impact from PV systems. It will also collect data for installed PV systems to analyze the trends to better understand how to handle the development. The models will be subjected to different scenarios for short circuit analysis, load flow analysis, and harmonic distortion simulations.

The thesis constructs the following chapters as:

- Chapter 2 - Theory relevant for PV systems in the distribution grid such as the electrical grid, voltage quality, low voltage production, and PV systems. The chapter introduces simulation tools, sensitivity analysis, and different measures to the grid.
- Chapter 3 - Methodology for data acquisition for PV system trends and consumption data, modeling circuits in PowerFactory, and simulation of study cases with different analyzing tools.
- Chapter 4 - Simulation results for different study cases to review the impact of PV systems and a comparison of the results.
- Chapter 5 - Discussions will consider the necessary assumptions and the robustness of the simulations. It will consider the general PV capacity for rural areas and the future trends of prosumers.
- Chapter 6 - Conclusion describes how to find the PV capacity of a low voltage grid in rural area and a method to handle new PV systems for grid planners. There will also be a recommendation for further work.

# 2 Theory

This chapter describes the relevant theory and consists of five parts. The first part is about the grid, power flow and fundamental grid behaviour. The second part is PV systems and voltage quality. The third part is an introduction to different simulation tools. The fourth part is sensitivity analysis for grid systems, and lastly, a description of different measures to preserve good voltage quality.

## 2.1 Electrical grids, power and energy

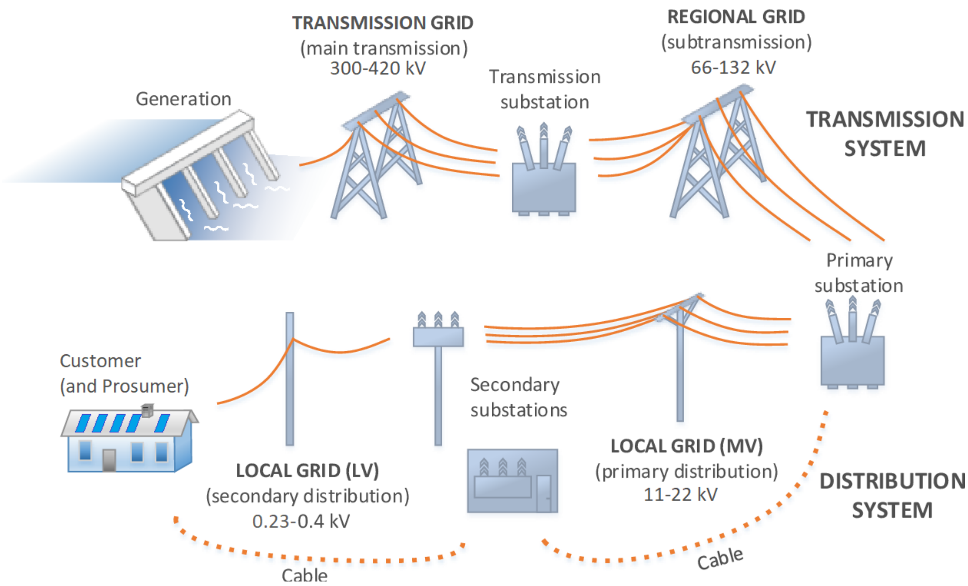


Figure 2.1: Overview of the Norwegian power grid [7].

The Norwegian power grid can be categorized into three parts, based on the voltage level. A general overview is shown in figure 2.1.

- Transmission grid (Normally 300 to 420 kV).
- Regional distribution grid (Normally 66 kV to 132 kV).

- Local distribution grid (Normally 0,23 kV to 22 kV) There are about 100 DSO in Norway. This grid is often divided into high voltage (11 kV to 22 kV) and low voltage (0,23 kV IT (Isolated terra) or 0,4 kV TN (Terra neutral)).

Two components make the Norwegian power grid different from most countries. The electricity production almost exclusively consists of hydropower plants and IT network is still dominant in the low voltage distribution grid [8].

Traditionally the grid has been a one-way road for power flow. Big hydropower plants produce and deliver electricity at higher voltages. The higher voltages are distributed closer to the loads and then transformed down to the end-users. Distributed generation was first commercially introduced in the 90s, as micro hydro power plants were installed and connected to the distribution grid at the high voltage side. Before PV systems, production in the low voltage grid was uncommon, and now PV system is the dominant production unit at the lowest voltage levels. If a customer with a PV system produces more electricity than he or she consumes, the power flows from the connection point and delivers electricity to the grid. If the production in a substation circuit surpasses the consumption of the circuit, then power would flow out to the high voltage grid [6]. Figure 2.2 shows an illustration of how the customer is connected to the grid. Main supply fuse limits the customers' consumption and production. The AMS smart meter measures the customers' consumption and production. This figure shows a customer connected to a substation through a cable cabinet. Customers can be directly connected to the substation without a cable cabinet or connected to the substation with overhead lines on poles. The interface between the DSO and the customer is often called the PCC (Point of common coupling) [9].

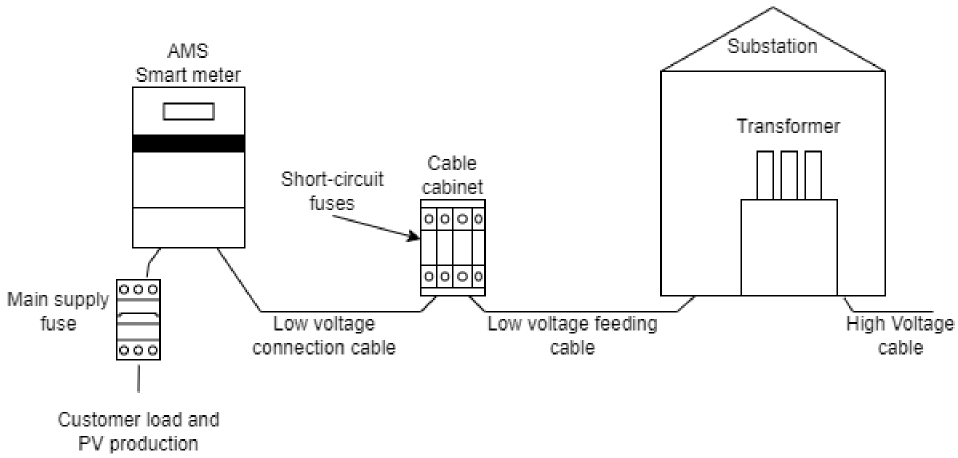


Figure 2.2: Illustrated overview of how the customer is connected to the grid.

### 2.1.1 A dynamic distribution grid with AMS

Many existing substation circuits takes account for up to 20 % voltage drop from the substation to the last customer. Most substations are set to give an output voltage of about 245 V IT and 425 V TN. A high output voltage gives a good margin for voltage drop from the substation to end-users at heavy load. The Norwegian regulations requires the DSO to keep the voltage variations for to be within ±10 % for customers [10]. PV systems may in periods cause voltage rises, the substations must therefore account for voltage drop during heavy load and voltage rise from PV systems. Both new and older customers can install PV systems; hence all new and old substation circuits need to account for this [6].

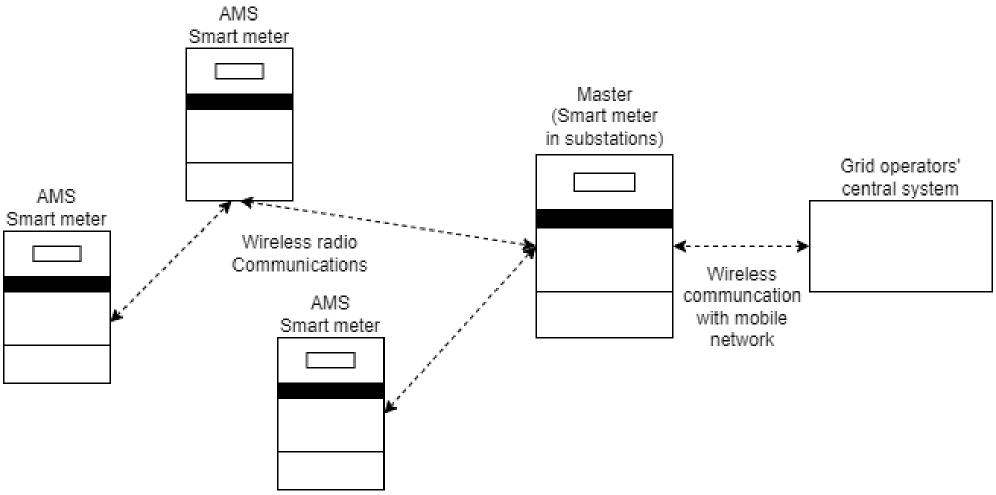


Figure 2.3: Illustrated overview of Advanced Metering Infrastructure [11].

All Norwegian DSOs have rolled out smart meters ”AMS” (Advanced Metering- and Control-system) too their end-users [12]. These new smart meters offer a more accurate measuring of consumption, production, and voltage [4]. The location of smart meters are close to the PCC. Figure 2.3 illustrates how the two ways communication between the smart meters and the DSOs’ central system. The AMS meters communicate with a master using radio communication, and the AMS meter can use other AMS meters as a signal extender in areas with bad connections. The masters use a mobile network to communicate with the DSOs’ central system work [13].

The AMS smart meter must according to regulation be capable of [4]:

- Storing measured values with a registration frequency of a maximum of 60 minutes and be able to decrease the registration frequency down to a minimum of 15 minutes.
- Connecting to a standardized interface that accounts for communication between external equipment based on open standards.

- Connecting and communicating with different types of meters (gas, heat, etc.).
- Shutting off or reducing the total load at a customer. The exception is for larger installations that uses current transformers for measuring.
- Sending and receiving information about power prices and tariffs, and be able to transmit control fault signals and earth fault signals.
- Registering the flow of active and reactive power in both directions.

### 2.1.2 Reversed power flow and voltage rise

Reversed power flow happens as the PV system produces more power than the customer consumes, and the excess power distributes to the grid. Figure 2.4 shows that production $P_G + Q_G$ is greater than consumption $P_L + Q_L$, causing the current $I_1$ to flow from the customer to the grid. The voltage drop over the cables' impedance $Z$ (resistance $R$ and reactance $X$) is now from customer $U_2$ to substation $U_1$, this can be defined as a voltage rise. The voltage rise depends on the power distributed to the grid and the strength of the grid. Short circuit current can represent the last parameter.

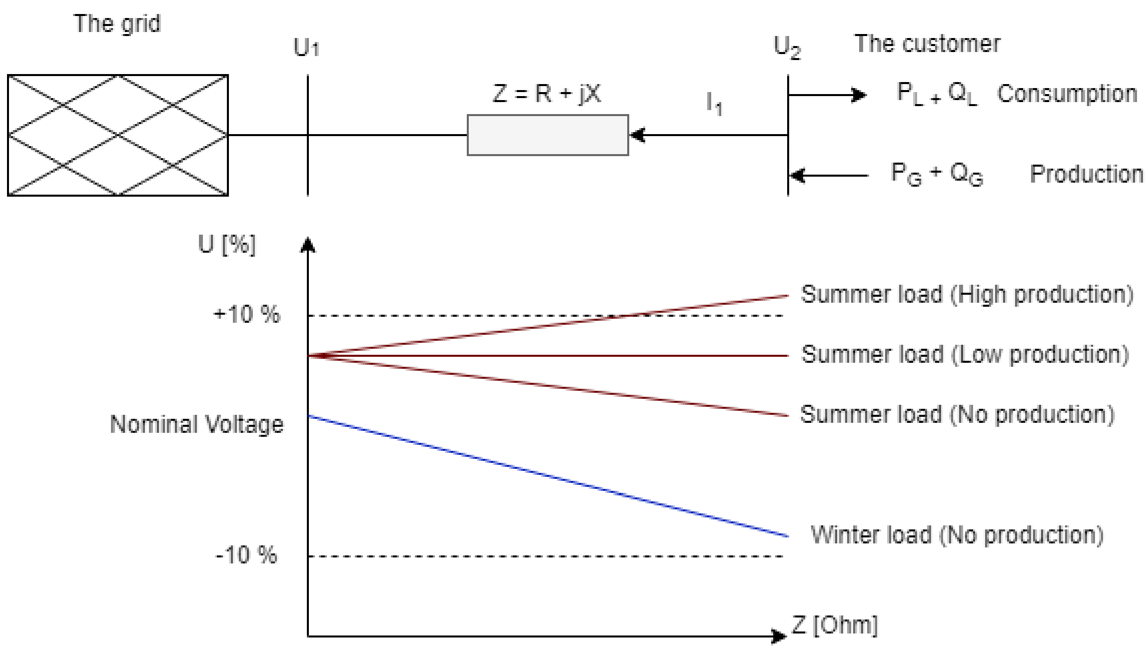


Figure 2.4: Simplified illustration of distribution with consumption and production.

The grid can encounter some problems with reversed power flow. If the production is high enough and the impedance is small enough, the voltage could be elevated and surpass the regulated limits. If the production power is greater than the thermal limit of the cable or transformer, then a component could be thermally overloaded, or protective relays could trip [5], [14].

### 2.1.3 Diversity factor and coincidence factor

A definition of diversity factor by Khare, Nema, and Baradar is "Diversity factor is as the ratio of the sum of the individual maximum demands of the various subdivisions of a system (or part of a system) to the maximum demand of the whole system (or part of the system) under consideration" [15]. All customers do not peak their load simultaneously. Therefore, the total sum of individual maximum load demand is greater than the maximum peak load of the system. Equation 2.1 shows how the diversity factor expresses the relation between individual maximum demand and the maximum demand of the system. The diversity factor will normally be more than one.

$$\text{Diversity Factor} = \frac{\text{Sum of individual maximum demand}}{\text{Maximum demand of the system}} \tag{2.1}$$

The coincidence factor is the reciprocal of the diversity factor. Bayliss and Hardy describe that some engineers prefer to describe a diversity factor to be between zero and one, the coincidence factor is the inverse of the diversity factor, as shown in equation 2.2 [16]. Bayliss and Hardy states that a coincident factor is always less than one and a general factor tends to settle at 0,3, at between thirty to unlimited number of loads. This is verified in the thesis of Lian, he measured the coincidence factor with AMS smart meters for a group of apartments to be as low as 0,3-0,4 [17]. This means that even though all customers have access to 100 % of their given capacity, only 30 % to 40 % of assigned capacity is used simultaneously.

$$\text{Coincidence factor} = \frac{1}{\text{Diversity factor}} \tag{2.2}$$

The coincidence factor is of great importance for distribution planning engineers as it is a key factor for the economic sizing of power grid components [16]. To reduce the cost of building a grid, engineers will use the coincidence factor to build the grid to handle the highest expected load in the future instead of the highest theoretical load. In most cases, the value of the coincidence factor cannot be measured and must be estimated. If the coincidence factor is estimated too high, the grid will be more expensive than needed. However, estimating the coincidence factor is too low, and the grid will not be able to handle the actual load. This leads to a higher risk of thermal overload in power grid components.

Coincidence factors and diversity factors can be adapted for PV systems. The PQA report states that the peak of production for a PV system is when the sun is pointing directly at PV panels. As the orientation and angle of the roof are different for buildings, the peak happens at different times. In regions where all roofs face the same way and have equal roof angles, the peaks would overlap, and the coincidence factor would be close to 1. In the PQA report, it is generally more common to assume a factor of 0,8-0,9 [6]. As the coincidence factor for PV systems are higher than for loads, there is a risk of thermal overload in areas with high PV penetration.

### 2.1.4 Thermal limitations in grid

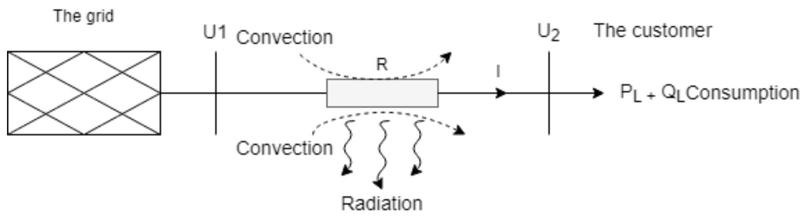


Figure 2.5: Simplified illustration of thermal loading in cable.

As a conductor with resistance conducts an electric current, some power converts to heat; this is called conductor-losses. Figure 2.5 illustrates the thermal loading of a simple circuit where the current $I$ flows through the line or cable resistance $R$ in $[\Omega]$ and to the load $P_L$ in $[W]$. The conductor-loss is defined in equation 2.3 [18]:

$$P_{\text{loss}} = I^2 \cdot R \tag{2.3}$$

Where the power loss, or the conductor-loss is $P_{loss}$ in $[W]$ is a product of resistance $R$ in $[\Omega]$ and current $I$ squared in $[A^2]$. The current depends on the customer load $P_L$, hence the conductor-losses varies with the consumption of the customer. The energy release of heat into the surroundings is shown in equation 2.4:

$$E_{\text{in}} = P_{\text{loss}} \cdot t \tag{2.4}$$

Where the energy release $E_{in}$ in $[J]$ is the conductor-loss $P_{\text{loss}}$ in $[W]$ over time, $t$ in $[s]$. The increased temperature of a mass is given in equation 2.5 [18]:

$$T_n = T_{n-1} + \frac{Q_E}{m \cdot C_p} \tag{2.5}$$

Where the increased temperature a mass $T_n$ in $[K]$ is the sum of the previous temperature of a mass $T_{n-1}$ in $[K]$ and the quotient of energy stored in the mass $Q_E$ in $[J]$ and the product of mass $m$ in $[kg]$ and specific heat capacity of the mass $C_p$ in $[J/(kgK)]$ [18]. The energy stored in the conductor is shown in equation 2.6 [19]:

$$E_{(\text{conductor})} = Q_E = E_{\text{in}} - E_{\text{out}} \tag{2.6}$$

Where the energy stored in the conductor $E_{(\text{conductor})}$ in $[J]$ is given by subtracting the energy release from conductor-loss $E_{\text{in}}$ and the dissipating energy from the conductor to the surroundings $E_{\text{out}}$ using radiation, conduction, and convection. Considering only heat dissipates to the soil and air, the heat release to surroundings neglects conduction. The equations 2.7 and 2.8 shows the heat release using convection and radiation [18], [19]:

$$E_{(\text{convection})} = h \cdot A \cdot (T_{n-1} - T_0) \cdot dt \tag{2.7}$$

$$E_{(\text{radiation})} = \varepsilon \cdot A \cdot \sigma \cdot ((T_{n-1})^4 - (T_0)^4) \cdot dt \tag{2.8}$$

Where the energy release using convection $E_{(\text{convection})}$ in $[J]$ is a product of the convective heat transfer coefficient $h$ in $[W/m^2K]$, the surface area of the conductor $A$ in $[m^2]$, and the temperature difference in $[K]$, all over time, dt in $[s]$. $T_0$ is the ambient temperature of the surroundings in $[K]$. The energy release using radiation $E_{(\text{radiation})}$ in $[J]$ is the product of the emissivity for the conductor material $\varepsilon$, the Stefan-Boltzmann constant $\sigma$ in $[W/m^2K]$ and the difference of temperature in $[K]$ in the power of four, all over time, dt in $[s]$. By inserting the equation 2.6 for stored energy in conductor into the equation 2.5 for temperature rise of a mass, the temperature of a conductor can be derived as, see equation 2.9 [18], [19]:

$$T_n = T_{n-1} + \left( \frac{E_{\text{in}} - E_{\text{out (convection)}} - E_{\text{out (radiation)}}}{m \cdot C_p} \right) \tag{2.9}$$

The full equation 2.10 by inserting equations 2.7 and 2.8 is shown under [19]:

$$T_n = T_{n-1} + \frac{I^2 \cdot R \cdot dt - (h \cdot A \cdot (T_{n-1} - T_0) \cdot dt - (\varepsilon \cdot A \cdot \sigma \cdot ((T_{n-1})^4 - (T_0)^4))) \cdot dt}{m \cdot C_p} \tag{2.10}$$

Equation 2.10 does not account for the change in cables and lines resistance with temperature. As temperature change, the resistance should be updated accordingly to equation 2.11 [8]:

$$R_n = R_{n-1} \cdot (1 + \alpha \cdot (T_n - T_{n-1})) \tag{2.11}$$

Where the resistance according to new temperature is $R_n$ in $[\Omega]$, it is the product of previous resistance $R_{n-1}$ in $[\Omega]$, the temperature coefficient $\alpha$ in $[1/K]$ and the temperature difference in $[K]$.

All cables and lines have a thermal limit. The thermal limit is given in temperature, and in rated current at ambient temperature. The conductor will reach its thermal limitations if the current is high enough in a given cable. Transformers have thermal limitations as the windings consist of conductors. It is essential to differentiate between the thermal limit for continuous stress and the thermal limit for specific time intervals. Continuous stress typically have a time span of more than an hour and is often caused by increased load or production. Thermal limit for specific time intervals typically have a time span of seconds or minutes and is often caused by short circuit current [8].

### 2.1.5 Short circuit current

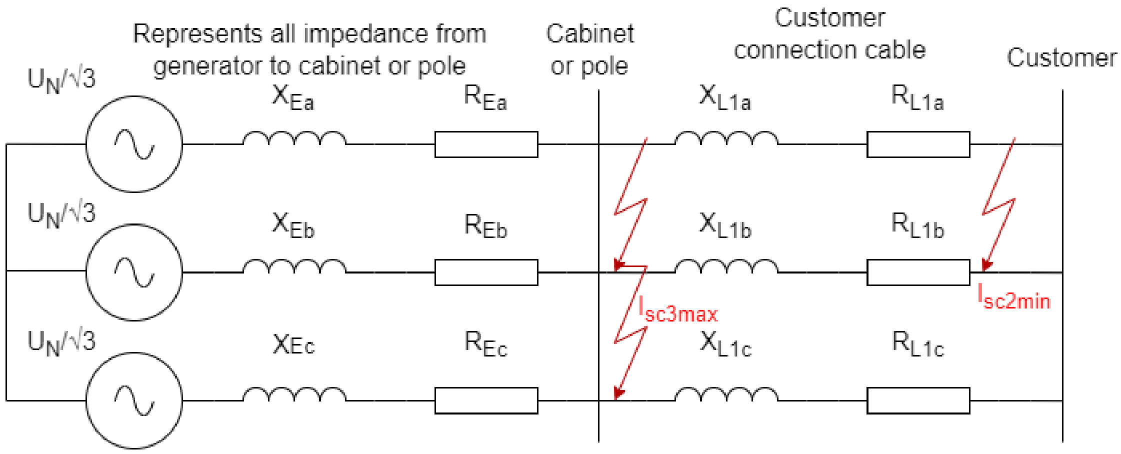


Figure 2.6: Simple illustration of a circuit with two types of short circuits for a customer connection cable.

Svarte defines *short circuit* in a three-phase grid as a characteristic by which the conductors in a system are connected over an impedance much smaller than the load impedance during normal situations [8]. The current in a short circuit is much higher than the current in a normal situation. Figure 2.6 shows a simple illustration of a circuit with a short circuit. The figure illustrates the maximum three-phase short circuit current $I_{sc3max}$ in $[A]$ and the minimum two-phase short circuit current $I_{sc2min}$ in $[A]$ for a customer connection cable. REN states that when a customer connects to the grid, the DSO should provide the maximum three-phase short circuit current and the minimum three-phase short circuit current [20]. The maximum three-phase short circuit current $I_{sc3max}$ is provided to ensure that the customers' relay has a high enough short circuit rating and can handle the energy from a short circuit event. $I_{sc2min}$ is provided together with the DSO short circuit fuse to ensure that the customers' short circuit relay is selective and disconnects in the event of a short circuit [21].

$$I_{sc3max} = \frac{U_N}{\sqrt{3} \cdot \sqrt{(X_E)^2 + (R_E)^2}} = \frac{U_N}{\sqrt{3} \cdot Z_E} \tag{2.12}$$

$$I_{sc2min} = \frac{U_N}{2 \cdot \sqrt{(X_E + X_{L1})^2 + (R_E + (R_{L1})^2}} = \frac{U_N}{2 \cdot Z} \tag{2.13}$$

The equations 2.12 and 2.13 corresponds to the figure 2.6. The inertia of generators in bigger power plants defines the power sustaining a short circuit current. The reactance $X_E$ and the resistance $R_E$ are the total impedance in $[\Omega]$ from cabinet or pole towards the generators. The reactance $X_L$ and the resistance $R_L$ are the impedance in $[\Omega]$ from the cabinet or pole to the PCC. The $U_N$ is the rated voltage in $[V]$. Svarte describes the equations and figures further in his subject book [8].

PQA states in their report that short circuit values can be used as a measure of grid stiffness [6]. The equations 2.12 and 2.13 show that if the short circuit current in a circuit is high, then the impedance value would be small. A low impedance value generally corresponds to high-capacity cables or lines or being close to the substation. These factors describe a stiff grid. If the short circuit current value is low and the impedance value is high. A high impedance value is generally caused by low-capacity cables, connection point being far away from the substation or a combination, which corresponds to a weak grid.

In a short circuit fault, it is vital with sufficient short circuit currents to ensure relays and fuses disconnect when a fault occurs in the grid. The short circuit currents can become very small for customers in weak grids, causing the short circuit fuses not to disconnect during a short circuit event. REN describes this problem in REN 8072, and in the same manual, the table 2.1 is found. The table shows the highest short circuit fuses that still disconnect at the given minimum two-phase short circuit current $I_{sc2min}$ [21].

Table 2.1: Smallest short circuit fuses that still ensures disconnection at given minimum two phase short circuit current [21].

| short circuit fuses [A] | $I_{sc2min}$ [kA] |
|---|---|
| 35 | 0,12 |
| 50 | 0,18 |
| 63 | 0,24 |
| 80 | 0,33 |
| 100 | 0,43 |
| 125 | 0,53 |
| 160 | 0,69 |

## 2.2 Voltage challenges from prosumers with PV systems

NVE-RME (The Norwegian Energy Regulatory Authority) manages the regulations regarding electricity in Norway. They define a *prosumer* as an end-use-customer with consumption and production of electric energy. This term does not apply to a generation that requires a license or generators that supply electricity to other end-users or if the prosumer at some time delivers more than 100 $kW$ [3]. If a grid has multiple prosumers, the degree of prosumers is often called PV penetration and can be calculated as shown in equation 2.14:

$$\text{PV penetration} = \frac{\text{Amount of prosumers in circuit}}{\text{Total number of customers in circuit}} \tag{2.14}$$

The PV penetration degree is derived from dividing the number of prosumers in the circuit by the total amount of customers in the circuit.

### 2.2.1 PV systems

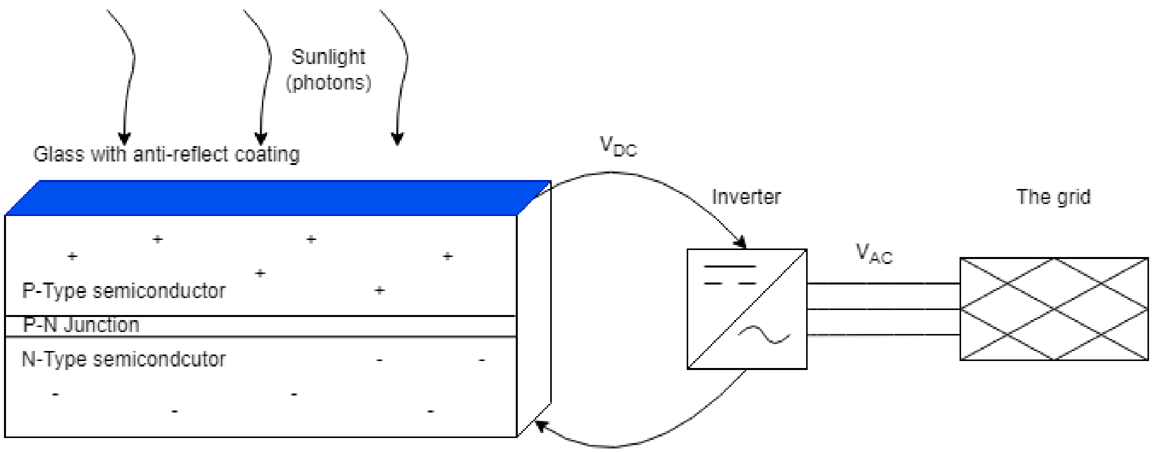


Figure 2.7: Illustration of grid-connected PV system.

The PV systems must have cables, measuring equipment, relays, switches, and an inverter to connect PV panels to the grid. Figure 2.7 shows an illustration of a grid-connected PV system from photons to input to the grid. Solar PV panels produce DC (Direct Current) by having doped semi-conductors to trap photons from the sun. The most common material for semi-conductor is silicon [22], [23].

A PV *inverter* is a power converter that most often consists of an IGBT (Insulated-gate bipolar transistor). IGBT consists of switches, normally with a switching frequency of between 2 and 20 kHz. The switching uses a PWM (Pulse width modulation) to convert the solar electric energy into a useful AC (Alternating Current) signal. The inverter reads the power grid, and the PWM matches the voltage, frequency, and phase angle. The switches can distort the grid; hence an inverter must be equipped with an EMC (Electromagnetic compatibility) filter or similar to decrease the distortion [5], [24]. The inverter is responsible for protecting itself from the grid by having anti-islanding protection, over- and undervoltage protection, and the opportunity to decrease or disconnect production by the DSO [5].

The deviation between actual and theoretical energy output is called PF (Performance ratio). In a report, Fraunhofer states that the PR for total PV systems is between 80 % and 90 % [25]. The PR is given in equation 2.15:

$$PR = \frac{E_{Grid}}{GlobInc \cdot PnomPV \cdot PV_{area}} \tag{2.15}$$

Where $E_{Grid}$ is the measured PV energy effectively delivered to the inverter $[kWh]$, $GlobInc$ is the incident irradiance in hourly values $[kWh/m^2]$, and $PnomPV$ is the PV panels rated efficiency factor in $[-]$, and $PV_{area}$ in $[m^2]$ [26].

### 2.2.2 Voltage quality

*Voltage quality* is the study on the different parameters that deviate from the ideal waveform of voltage. Deviations or disturbances can cause discomfort for customers and, in the worst case, damage electrical equipment [10].

Norwegian regulation of quality of electricity supply regulates three different terms of quality. The first term is continuity of supply. NVE-RME describes it as the availability of electrical energy, measured by the frequency and duration of the interruption. The second term is voltage quality, where voltage quality describes the applicability of electrical energy. Correct voltage magnitude and the waveform are vital for having usable electricity and then explained by REN [5], [27]. The third term is information service and contains the non-technically services such as customer service and information technology regarding the other two terms. This report will not further discuss the first term, continuity of supply, or the third term, information service. The definitions and values in this section are translated from the regulation of quality of electricity supply [10], [27]. The regulation specifies different measurable parameters for voltage quality in the list below:

- The frequency of the voltage
- Slow variations in the RMS (Root-Mean-Square) value of voltage

- Rapid voltage changes
- Flickering
- Voltage imbalance
- Over harmonic voltages
- Interharmonic voltages
- Transient overvoltages

#### Frequency

TSO (Transmission System Operator) controls the frequency by controlling the power production from larger power plants. Individual prosumers in the low voltage grid do not affect the power production in the grid to impact the frequency to a measurable degree [28]. However, findings in a report from Seneviratne and Ozansoy states that the frequency stability may severely decline due to prolific penetration from PV generators [29]. This thesis will not further discuss frequency as it focuses on the impact of PV systems in the low voltage distribution grid.

#### Slow variations in the RMS value of voltage

According to Norwegian regulation, the Norwegian DSO's are obliged to deliver electricity inside a range of ±10 % nominal voltage at the PCC. ±10 % is maximum 253 V and minimum 207 V for IT network and maximum 440 V and minimum 360 V in TN network. As mentioned in 2.1.2 a PV system with surplus production will increase the voltage. The voltage drop is shown in equation 2.16 and can also be used to calculate a voltage rise:

$$\Delta U = \frac{1}{U} \cdot [(P \cdot R - Q \cdot X) + I \cdot (P \cdot X + Q \cdot R)] \tag{2.16}$$

Where $\Delta U$ is the voltage drop or voltage rise in $[V]$ from one busbar to a second busbar. $U_2$ is the voltage in $[V]$ at the second busbar. $P$ in $[W]$ and $Q$ in $[var]$ are the active and reactive load or production at the second busbar. $R$ in $[\Omega]$ and $X$ in $[\Omega]$ are the resistive and inductive parts of the impedance of the cable that connects the busbars. One simplification is to neglect that as the voltage increases, the current will decrease which decreases the voltage drop or rise. This simplification removes the current part of the equation and the new equation 2.17 is:

$$\Delta U = \frac{(P \cdot R - Q \cdot X)}{U} \tag{2.17}$$

The second simplification assumes that the PV installation does not compensate for the reactive power. The impact by compensation of reactive power is limited as the ratio between resistance and reactance (R/X-ratio) is resistance dominant. This means the reactive part is small, and therefore the contribution of the reactive power can be neglected. The R/X ratio will be more reactive dominant closer to the substation or long distribution lines where the conductor has a big cross-section. This means that the simplification can have deviating results for cases closer to substation or with long, high cross-section lines [5]. From this simplification and equation 2.17 vi can extract the equations at table 2.2.

Table 2.2: Simplified equations for calculation of the voltage rise from single standing PV systems [6].

| Grid system | IT network | TN network |
|---|---|---|
| One-phase | $\Delta U = \frac{P_R}{I_{sc2}}$ | $\Delta U = \frac{\sqrt{3} \cdot P_R}{I_{sc2}}$ |
| Three-phase | $\Delta U = \frac{P_R}{2 \cdot I_{sc2}}$ | $\Delta U = \frac{\sqrt{3} \cdot P_R}{\sqrt{3} \cdot 2 \cdot I_{sc2}}$ |

Table 2.2 shows simplified equations for calculating the slow voltage variations. $\Delta U$ is the voltage rise from PV system, $P_r$ is the rated power of the PV system, and $I_{sc2}$ is a two-phase short circuit current at PCC. Based on the table and the report from PQA AS we can establish that [6]:

- Increasing the rated power of PV system $P_R$, will increase the voltage rise.
- A one-phase PV system has higher voltage rise than a three-phase PV system.
- Increasing the short circuit current $I_{sc2}$, will decrease the impact of the PV system on the grid.

The short circuit currents were discussed in section 2.1.5. It is essential to understand the difference between $I_{sc2}$ and $I_{sc2min}$. $I_{sc2min}$ is the value presented in the section, and it takes the temperature increase during a fault into account. Therefore it is about 1,3 smaller than $I_{sc2}$ [6], [30].

To counter the effect of voltage rise due to prosumers, the distribution transformer can tap down [5]. Tapping is to regulate the voltage by changing the winding ratio with a tap changer in the transformer [18]. Be aware that the set value of the tap changer could be high to ensure a high enough voltage accordingly to regulation for a customer with a low short circuit current [6]. The tap changer is also used when connecting a transformer to the high voltage grid. Because of voltage drops in high voltage grid, the output voltage may not be as high as nominal. The tap changer adjusts the low voltage to be correct.

### High voltage deviation

The voltage drops in high voltage distribution grid varies, this variation in the high voltage grid can affect the low voltage grid. The variation in voltage from the high voltage grid can be divided into two components. The first component is voltage drop from loads or voltage rise (caused by micro power plants, wind farms, or Ferranti effect). The report from PQA assumes from experience that high voltage variation is often around 5 % but can sometimes be as high as 7 % [6]. The second component is regulation from OLTC (On-Load Tap-Changer Controller) power transformer. Consider the tap-change controller in the power transformer, which automatically regulates the voltage of the busbar in the secondary station. The regulation is usually made in steps with a deadband of somewhere between 1 % and 3 % [6]. If the tap-changer controller made a perfect regulation of the voltage, the voltage variation in the high voltage grid would be equal to the deadband of the tap-changer controller. However as the power transformer distributes to multiple radials, and the losses are different for every radial, the variations in the high voltage grid must be higher than the deadband.

The sum of variations in the high voltage grid can therefore be around 2-8 %. REN recommends the DSO to have a 5 % limit of slow stationary high voltage variations, a tap-changer controller of 2 % is taken into account, which means that total high voltage variations up to 7 % can be expected [31].

### Voltage imbalance

Voltage imbalance is the difference in voltage values between phases. Norwegian regulation [10] § 3-6 states that the DSO is responsible to keep the voltage imbalance between phases below 2% in the PCC, measured as an average over ten minutes. The degree of voltage imbalance can be calculated as the relationship between the voltages positive $U_+$ and negative $U_-$ sequence components and is expressed in equation 2.18 [10]:

$$\frac{U_-}{U_+} = \sqrt{\frac{1-\sqrt{3-6\beta}}{1+\sqrt{3-6\beta}}} \cdot 100\% \tag{2.18}$$

Where $\beta$ is defined in equation 2.19:

$$\beta = \frac{U_{12}^4 + U_{23}^4 + U_{31}^4}{(U_{12}^2 + U_{23}^2 + U_{31}^2)^2} \tag{2.19}$$

Where the voltage values are the voltage measured between phases. Voltage imbalance occurs when there is an unbalance in load, and it could also occur with PV systems with a one-phase inverter. To decrease the likelihood for voltage imbalance the DSO Lede AS uses a connection agreement developed by REN. The agreement states that a PV system with rated current of 16 $A$ or more must use a three-phase inverter to decrease the possibility of imbalance [32].

#### THD and over harmonic voltages

Over harmonic voltages are varieties from the voltages sine wave outside in the 50 Hz frequency. Nonlinear loads causes over harmonic voltages by for instance high-speed switching to pick small parts from the voltages sine waves, causing the current not to be sinusoidal. Examples of nonlinear loads are AC-DC (Alternating Current to Direct Current) converters and other power electronics. Over harmonic voltages can be represented as integer times the fundamental frequency, for instance 50 Hz frequency has 100 Hz (2nd harmonic), 150 Hz (3rd harmonic), etc. The total effect of these harmonics up to the degree of 40th is expressed as THD (Total Harmonic Distortion).

The DSO is responsible to keep the THD at PCC below 8 % and 5 %, measured on an average over ten minutes and one week, for customers with nominal voltage from 230 V to 35 kV. Prosumers with more than 30 $kW_p$ installed capacity are only allowed to feed in a maximum of 70 % of the THD limit set by Norwegian regulation [10], [32]. Equations 2.20 and 2.21 shows how to calculate the THD [18]:

$$THD = \frac{I_H}{I_F} \tag{2.20}$$

$$THD = \frac{U_H}{U_F} \tag{2.21}$$

Where the THD is in [%], $I_H$ and $U_H$ are the effective value of all the harmonics in [$A$] and [$V$], respectively, and $I_F$ and $U_F$ are the effective value of the fundamentals in [$A$] and [$V$]. The effective value of all the harmonics is shown in the equation 2.22 [18]:

$$U_H = \sqrt{U_2^2 + U_3^2 + ... + U_n^2} \tag{2.22}$$

The DSO is responsible for keeping the individual over harmonic voltages below the following values in table 2.3, measured as an average over 10 minutes, in connection points with nominal voltage from 230 V to 35 kV.

Table 2.3: Limits for allowed individual harmonic voltages in connection point set by Norwegian regulations [10].

| Odd harmonic voltages | | | | Even harmonic voltages | |
|---|---|---|---|---|---|
| Non-multiple with 3 | | Multiple of 3 | | | |
| Order of h | U | Order of h | U | Order of h | U |
| 5 | 3,00 % | 3 | 3,00 % | 2 | 1,50 % |
| 7, 11 | 2,50 % | 9 | 1,50 % | 4 | 1,00 % |
| 13, 17 | 2,00 % | 15, 21 | 0,50 % | 6 | 0,50 % |
| 19, 23 | 1,50 % | >21 | 0,30 % | >6 | 0,30 % |
| 25 | 1,00 % | | | | |
| >25 | 0,50 % | | | | |

A Report from Ahsan, Khan, Hussain, Tariq, and Zaffar states that a high prosumer penetration causes more THD than circuits without solar power. Also, circuits with a low short circuit current are more exposed to over harmonic currents [33]. A report from Patsalides found that when solar irradiation is lowest, the harmonic current spectrum is highest. However, the total harmonic voltage distortion was highest at high irradiates, as the produced power was highest [22].

#### Interharmonic voltage

Interharmonic voltage is a voltage component of a periodic quantity with a frequency that is not an integer multiple with the operating frequency of the power system [34]. A report from Ravindran, Rönnberg, Busatto and Bollen states that PV system can produce interharmonic voltages in the grid. The interharmonic voltages are most common at the transition between the PV system producing and not producing, such as sunrise and sunset [35].

#### Transient overvoltage

Transient overvoltage, or spike, is a type of overvoltage in the grid. The voltages range from 1.3 pu and up to 3 pu, usually lasting a few microseconds. Examples of transient overvoltage are lightning or switching in transmission grid [36]. In a report, Zhang, Du, and Chen stated that a bolt of lightning to transmission lines nearby a PV system can impact the PV system. This stresses the importance of having overvoltage protection in PV systems [37].

### 2.2.3 Relays and impact from PV installations

Multiple units delivering electricity to the grid can cause problems for relays. PV systems need to have an anti-islanding relay to avoid producing and delivering electricity out on the grid when there is an outage. An anti-islanding relay reduces the risk for installers as they need to be sure that the installation is without voltage to work safely. There is a risk of malfunctions of relays when the PV system feeds current between the relays and the place of fault, and this is called blinding [38]. Another problem is if there is a relay between the PV system and the fault, the PV system might try to feed a fault with a short circuit current, resulting in sympathetic tripping [6]. Namangolwa and Begumisa state in their master thesis that many of these relay problems can be observed at a PV penetration of 30 % or more [39].

## 2.3 Simulation tools

PowerFactory is a power system analysis software created by DIgSILENT GmbH, that can recreate and simulate models of the grid. PowerFactory is the chosen analysis tool in this thesis because of the ability to do load flow analysis with PV systems, and harmonic flow analysis [40].

Trimble NIS is a geographical and technical documentation software, and the grid system of Lede AS is documented accordingly to geographical positions. This thesis uses Trimble to access the grid data from Lede AS. Trimble is a tool for grid planners as it can perform electrical calculations such as short circuit calculations and load flow analysis. Trimble can collaborate with other systems such as AMS [41].

### 2.3.1 Analyzing tools

This chapter have earlier described thermal limitations, short circuit current, and voltage rise. PowerFactory can simulate the thermal load of cables and transformers and the voltage at all nodes using load flow analysis. Figure 2.8 shows that by inserting the bus, lines, production, and consumption data, the load flow analysis can calculate the voltage, current, and power in the circuit.

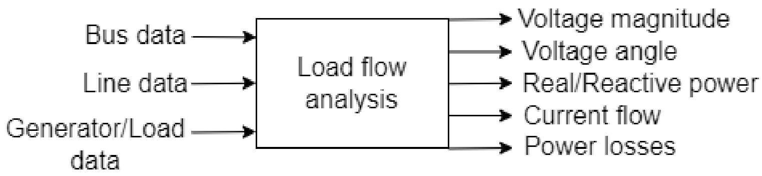


Figure 2.8: Flow chart of load flow analysis.

PowerFactory does the harmonic load flow calculation. By inserting the harmonic current spectrum into components in the circuits. Harmonic load flow can analyze the frequency-depended network impedances [42].

## 2.4 Sensitivity analysis

A sensitivity analysis is the study to find the uncertainty of an output of a system that can be divided into the uncertainty of different inputs. Sensitivity analysis can be used for decision making or development of recommendations for decision-makers. Inside this category, there are two subcategories suited to analyze the impact of PV systems in low voltage grid systems. One of which is identifying sensitive or essential variables. The second one identifies critical values, thresholds, or break-even values where the optimal strategy changes [43].

The outputs can be identified as measurable restrains in a power system, such as thermal overload, voltage level, and voltage distortion. The main contributors to thermal overload are impedance and current. The impedance is set by the cable type, the line type, the transformer type, and size. The load and production define the current.

The voltage level is set by feeding voltage from an overlying high voltage grid. The voltage varies with load and production in the overlying grid, regulated by an OLTC power transformer. The high voltage grid feeds the distribution transformer in the substation. The tapping level of the distribution transformer sets the base level of the low voltage grid. The voltage bandwidth of the end-users is then set by the variation in the high voltage grid and the low voltage bandwidth with voltage rise/drop between substation and end-user. The voltage rise or drop is set by the impedance of the cables and lines, which corresponds to the short circuit current.

Harmonic voltage distortion is described in subsection 2.2.2. Harmonic distortion is set by input from power electronics. From the perspective of power electronics, the impedance of the grid is frequency-dependent. The power electronic has a harmonic current spectrum, and these two parameters will create harmonic voltage distortion in different orders. Together these orders are total harmonic distortion. Therefore, the harmonic distortion is set by the power electronic apparatus and the impedance of the grid. Compared to voltage, the grid's impedance can also correspond to a short circuit current.

## 2.5 Measures to preserve voltage quality

REN describes some different methods to increase connection capacity in high voltage distribution. Methods such as upgrading the grid, shunt-reactor, series voltage regulators, automatic tap changer on distribution transformer, higher temperatures in line, and energy storage [44].

Voltage regulation with series regulators is a component placed far out in long and weak high voltage lines where all substations need counteracting for voltage regulation. There are also series regulators for low voltage grids, suitable for long low voltage grids with multiple consumers or prosumers. Series regulators are then used to have an extra flexible voltage bandwidth [45].

To preserve a sufficient voltage level in the low voltage grid, a distribution transformer with automatic tap-changer controller could be inserted in a substation to counter the high variation in a low voltage grid. The tap-changer controller shifts the voltage bandwidth by automatic tapping. The tap-changer controller can increase the substation voltage in wintertime with high load and decrease substation voltage in the summertime with low load and/or high production. One problem with automatic tap-changer controller is the control unit uses the substation voltage as reference, however the voltage problem happens at the customers [46].

Reactive power regulation is a method where the inverter consumes reactive power from the grid. This will reduce voltage rise. This method is most effective when the R/X-ratio is highly reactive dominant, which often means a customer must be close to a substation or is fed with overhead lines with big cross-section [47]. The effect of reactive power regulation can be limited in the case of customers in weak grids, as the R/X-factor is typically resistive dominant [48].

Curtailment is to pay a prosumer to limit delivery of electricity to the grid. The DSO can consider this in cases where the prosumer plans to produce and deliver a high amount of power where the power grid is weak. These cases would require the DSO to invest by upgrading the grid to handle the new production. Notice that this is not something the DSO can decide alone, this requires an agreement between the DSO and the customer [6].

Batteries in low voltage grid can be used for weak voltage grids with few customers. As the voltage rise is high, the battery charges, this will increase the load and decreasing the grid voltage. Vice versa, as voltage drops low, the battery can discharge, decreasing the load and increasing the voltage [49].

# 3 Methodology for grid simulations and sensitivity analysis

In chapter 2 the necessary theory for the grid, the PV system, and the voltage quality were described. Simulation tools and sensitivity analysis were discussed. Different measures to preserve voltage quality were introduced.

This chapter is divided into three parts. The first part describes the mapping of PV systems trends, the second part models the different study cases, and the last part defines the study methods.

## 3.1 Data acquisition

Three sets of data are acquired to analyze the consequences and trends of PV installations in the grid of Lede AS. The first set with data is all installed PV systems in Lede AS grid. The second set with data is data of all low voltage grids in the area of Lede AS to get an overview of Lede AS situation today. The last set with data is to collect data on consumption, production, and voltage regarding prosumers and customers for relevant circuits.

It is vital to note that GDPR (General data protection regulation) regulates customers' privacy. Therefore it is necessary that all data used and given in this report is not recognizable back to the customers.

### 3.1.1 Network connection message

According to Norwegian regulations, all customers must report to the DSO with a network connection message when installing a PV system with a higher capacity than 0,8 $kW_p$ in their installations [50]. The trend of installing PV systems is found by sorting these messages by year, amount, and size. The report finds relevant cases for simulation and interprets the future trends for PV installations by using these messages.

Table 3.1 shows the implementation of PV systems in Lede AS grid area per year and size for the last four years. The table shows an increase in average size, total size, and the

Table 3.1: Total installed PV system for Lede AS operating area (installations under 100 $kW$).

| Year | Number | Total installed power [$kW_p$] | Average installed power [$kW_p$] |
|---|---|---|---|
| 2017 | 52 | 471.28 | 9.06 |
| 2018 | 103 | 1017.37 | 9.88 |
| 2019 | 233 | 2087.90 | 8.96 |
| 2020 | 234 | 3457.87 | 14.78 |
| 2021 | 215 | 2876.4 | 13.385 |

total number of installed PV systems. The data from Lede AS is only for the past four years. This thesis needs to use data from NVE to get a clearer idea of the development of PV system trends. The figure 3.1 from NVE (The Norwegian Water Resources and Energy Directorate) shows the development of PV systems in Norway over the last 21 years. The different colors in the figure are a distribution of the sizes. The figure shows no records of PV systems before 2014 but a significant increase from 2014.

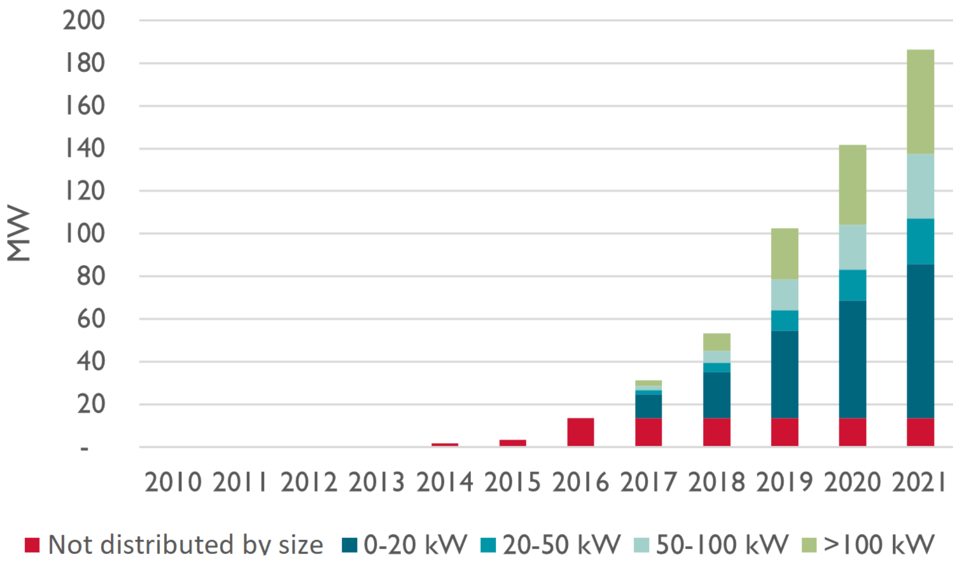


Figure 3.1: Development of grid-connected PV systems in Norway from NVE [3].

## 3.2 Modeling of distribution grid

Different circuits in the grid can be categorized as rural or urban, industrial or domestic. The report from PQA states that rural areas with older distribution circuits were the type of grid with the most challenges connecting multiple PV systems [6]. Traditionally only IT networks were built, and therefore four different rural IT networks will be further considered in this report.

The grid model starts from the high voltage connection and ends at each end-user on a given circuit. The grid beyond the high voltage connection is considered the external grid. The external grid model uses the short circuit currents calculated for the high voltage cable to the substation and calculated output voltage to the substations. The harmonic distortion model uses the harmonic distortion measured using AMS. According to measured values, the THD was around 1 to 1,5 % for all circuits.

The models use an assumed value of 4 % variation in the high voltage grid. This represents both the high voltage grid losses and the deadband from OLTC power transformer.

The model of distribution transformer uses Trimble NIS data for transformers, which again originates from the transformers data sheet. The data can be found in appendix C.

The busbars are nodes in the circuit, and points in the grid measuring the voltage. The busbar represents transformer busbars, cable cabinets, and poles where branches divide or customers are connected. Losses from busbars and connection points are not considered.

The lines and cables models use Trimble NIS data. Trimble NIS transfers a list with types for every cables and lines to PowerFactory. The data sheet includes resistance and inductance per kilometer, the current limit, and is shown in appendix C. The length is collected from Trimble NIS and inserted for every element in PowerFactory. Table 3.2 shows the short circuit currents for circuit 1 calculated by Trimble and PowerFactory. The short circuit results show that the external grid, transformer, cables, and lines are comparable, as the results are approximately equivalent, see appendix D.

Table 3.2: Short circuit current for circuit 1 calculated in Trimble NIS and PowerFactory.

| | Trimble NIS | | PowerFactory | |
|---|---|---|---|---|
| | $I_{sc2min}$ | $I_{sc3max}$ | $I_{sc2min}$ | $I_{sc3max}$ |
| Customer 1 | 387 | 605 | 387 | 606 |
| Customer 2 | 1185 | 1738 | 1115 | 2655 |
| Customer 3 | 536 | 811 | 529 | 822 |
| Customer 4 | 450 | 678 | 438 | 677 |
| Customer 5 | 196 | 306 | 184 | 289 |
| Customer 6 | 762 | 1120 | 793 | 1217 |

PV system uses rated peak power value for simulation. It assumes no diversity factor between prosumers production, the PF of PV systems is set to 100 %, and the power factor, cos phi is set to 1. To simulate harmonic distortion from PV systems, the PV system model uses a harmonic current spectrum presented in a report from Patsalides [22]. The report presents the harmonic current spectrum from cases with different levels of irradiates. The spectrum has the highest values at low irradiates, but the distortion is highest at high irradiates because the high power at high irradiates supplies power to the distortion. Figure 3.2 shows the harmonic current spectrum with accompanying angles from a 16 $kW_p$ PV system at high irradiates and is further used in this report.


(a) Amplitude in [A].

(b) Angle in degrees

Figure 3.2: The harmonic current spectrum for a 16 $kW_p$ PV system at high irradiates [22].

Figure 3.3 shows how a substation circuit is represented in Trimble NIS. It is the same circuit as study case 1, which will be used later in this report. The red lines are the high voltage overhead lines, and the dotted red line is the high voltage cable. The light blue lines are the low voltage overhead lines. The green lines are the low voltage cables.

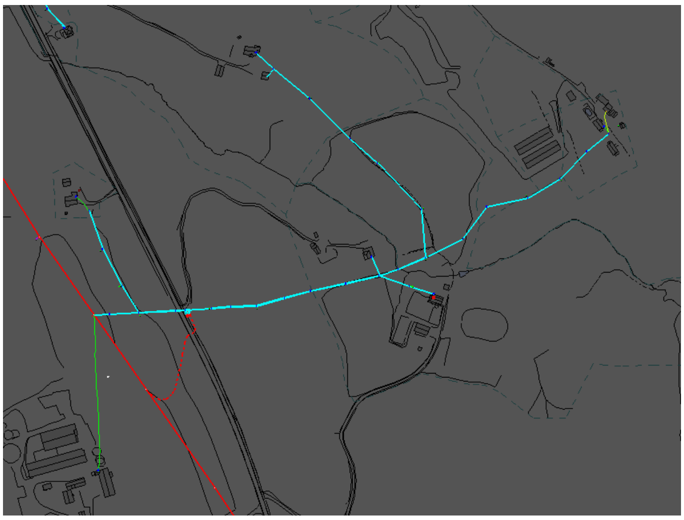

Figure 3.3: Map of a substation circuit in Trimble NIS.

### 3.2.1 Modeling of consumption

All customers have an AMS smart meter, and the meter collects the consumption data for every customer. The representative consumption value uses the measured average total power consumption per hour. The smart meter measures the THD in the circuits, and the THD is used to model the background harmonic distortion in the external grid.

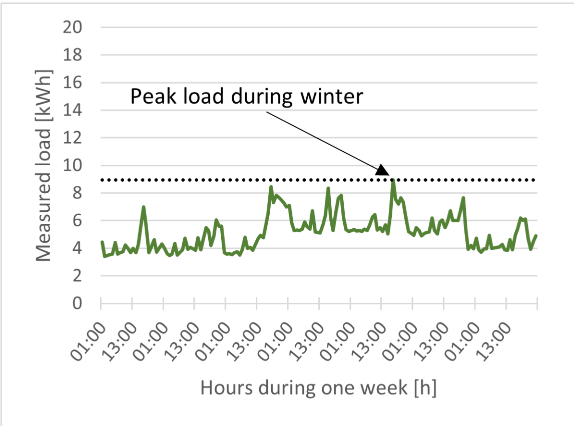


(a) Highest measured load in a week during winter time for customer.

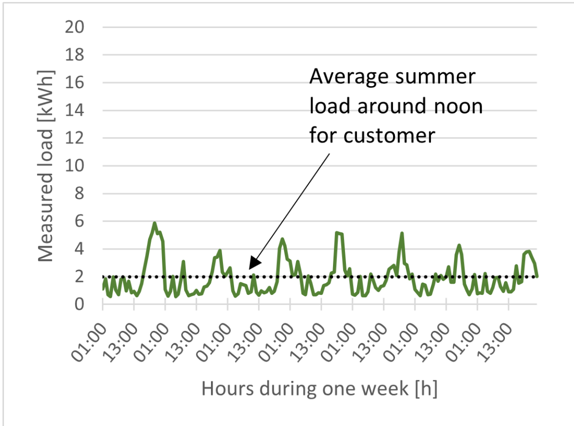


(b) Average low load measured in a week during summer time for customer.

Figure 3.4: The green lines are measured consumption with hourly values over a weak. The dotted lines are the chosen consumption value to represent the circuit.

In figure 3.4 the winter load is shown to the left-hand side and is the week with the highest measured consumption for a customer. The highest load for this customer was found in week 5 of 2021. The representative consumption value uses the peak load from the records. The chosen value is conservative as the event only have been measured once. In figure 3.4 the summer load is shown on the right-hand side and is chosen from week 34 of 2021. The chosen value is an average of around noon in the summer. This value is more realistic, as it is measured multiple times throughout the year. The load values have the unit *kVA* (kilo-volt-ampere), and the power factor cos phi is set to 0,9.

In the chosen study case, all cases have at least one prosumer. The choice of consumption profile for prosumers is slightly different, as they need to consider the existing PV system. Figure 3.5 shows measured power values for a prosumer in a green line and the chosen consumption value in a dotted black line. The representative consumption value for winter load is chosen the same way for a prosumer, as for a customer. The representative consumption value for summer load is chosen as an average value from the evenings. The summer load for a prosumer will be selected slightly higher than customer. The represented consumption value for a prosumer should be as if there was no PV system there.

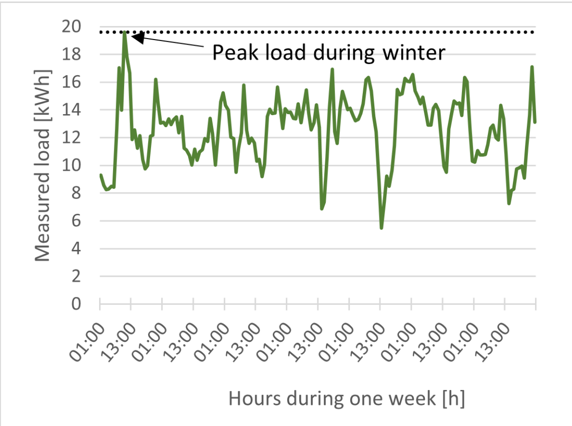


(a) Highest measured load in a week during winter time for prosumer.

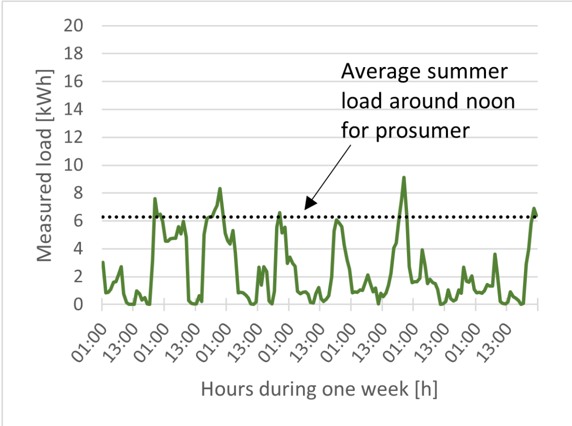


(b) Average low load measured in a week during winter time for prosumer.

Figure 3.5: The green lines are measured power consumption for a prosumer with a 16 $kW_p$ PV system with hourly values over a weak. The dotted lines are the chosen consumption value to represent the circuit.

The thesis will use this described procedure to find representative consumption values for all customers and prosumers as the study cases will be defined in the next sections. The figures of PowerFactory models are also shown in appendix B.

### 3.2.2 Study case 1

Figure 3.3 is the study case 1 in Trimble. PowerFactory uses the circuit in Trimble to create a model in PowerFactory. Figure 3.6 shows the model of study case 1 in PowerFactory.

The circuit is in a rural area with six customers, and the distribution transformer is 100 $kVA$. There is one customer in this circuit with a critical low $I_{sc2min}$ of 186 A. The voltage drop from the substation to this customer in the wintertime is 27 V or almost 0,12 pu.

Figure 3.7 shows the voltage drop for the circuit, and the blue line is winter load. All customers have a higher load in this situation, and therefore the voltage drop is more significant than the summer load. The red lines are summer load. In the x-axis, the number 1 is the substation node, so the blue and red lines show the voltage at the substation in the begging. The customers' voltage is at the end of the lines, and the connection points between the substation and the customer are nodes, such as cable cabinets and poles.

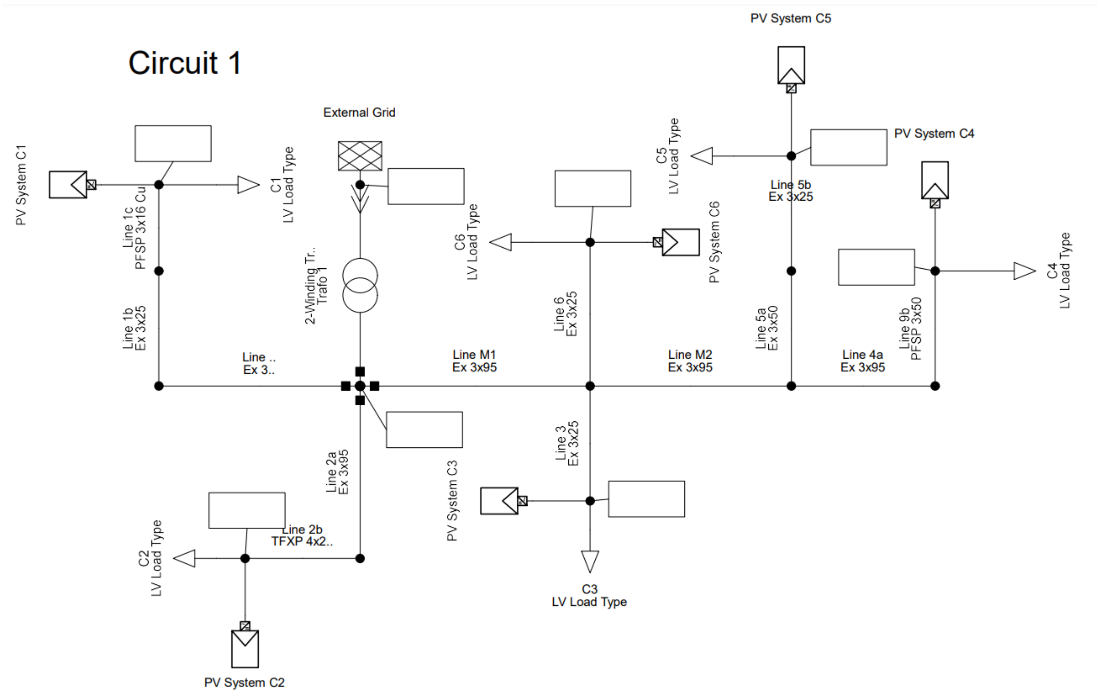


Figure 3.6: Substation circuit 1 represented in PowerFactory.

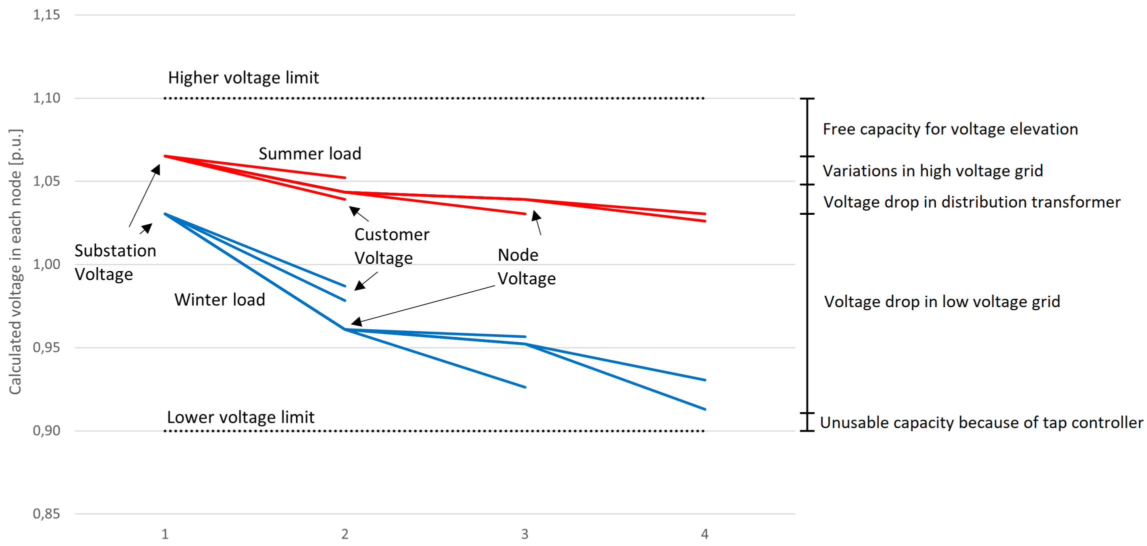


Figure 3.7: Voltage drop for circuit 1 in summer time (red) and winter time (blue) without PV systems.

### 3.2.3 Study case 2

Figure 3.8 shows the PowerFactory model of study case 2. The circuit has ten customers, and the distribution transformer is 100 $kVA$.

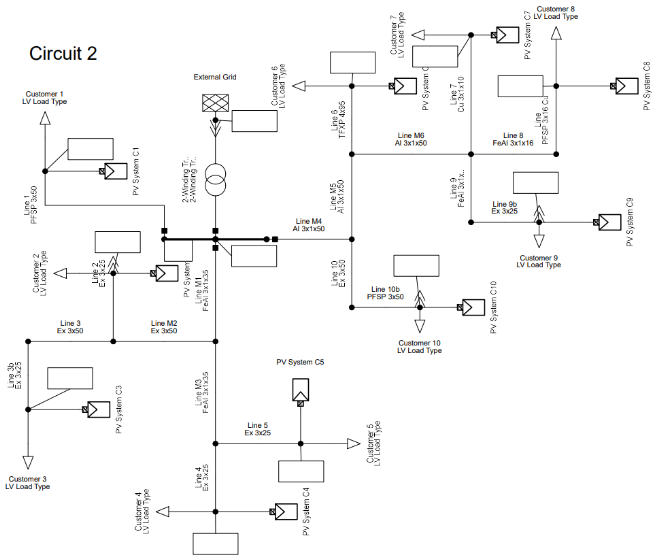


Figure 3.8: Substation circuit 2 represented in PowerFactory.

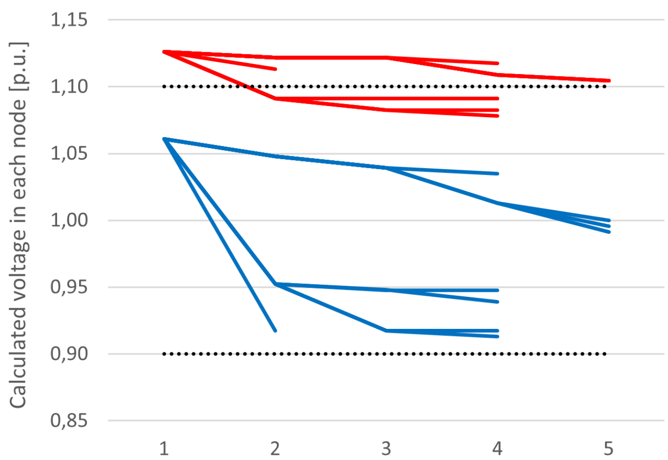


Figure 3.9: Voltage drop for circuit 2 in summer time (red) and winter time (blue) without PV systems.

Figure 3.9 shows the voltage drop for summer and winter load in circuit 2. The voltage drop is significantly bigger than circuit 1. The customer with the weakest grid has a $I_{sc2min}$ of 262 A, and the biggest voltage drop during wintertime is 34 V or almost 0,15 pu. The summer load is outside the limits because of a big difference in load between winter and summer and a 4 % variation in the high voltage grid.

### 3.2.4 Study case 3

Figure 3.10 shows the PowerFactory model of study case 3 with six customers, and the distribution transformer is 50 $kVA$.

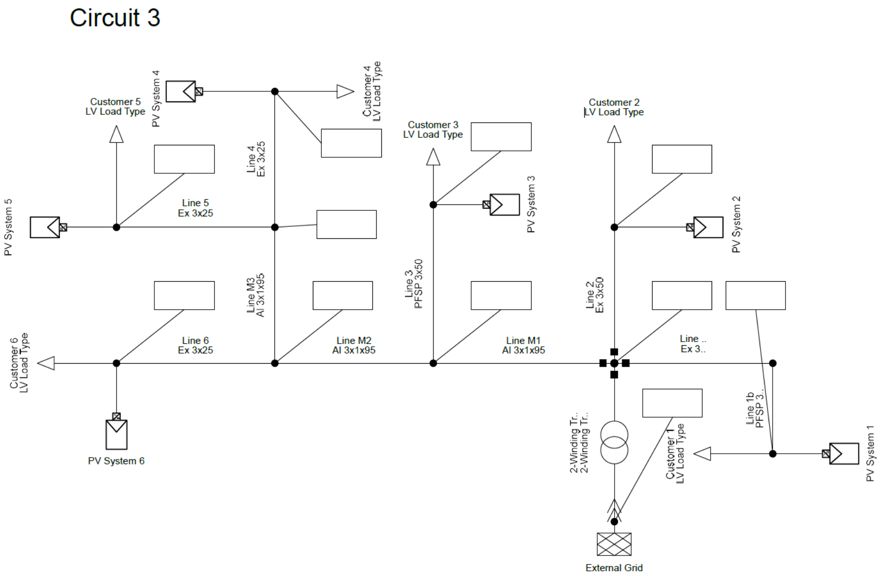


Figure 3.10: Substation circuit 3 represented in PowerFactory.

Figure 3.11 shows the voltage drop with summer and winter load. The customer with the weakest grid has a $I_{sc2min}$ of 530 A, and a voltage drop of 11 V or 0,05 pu.

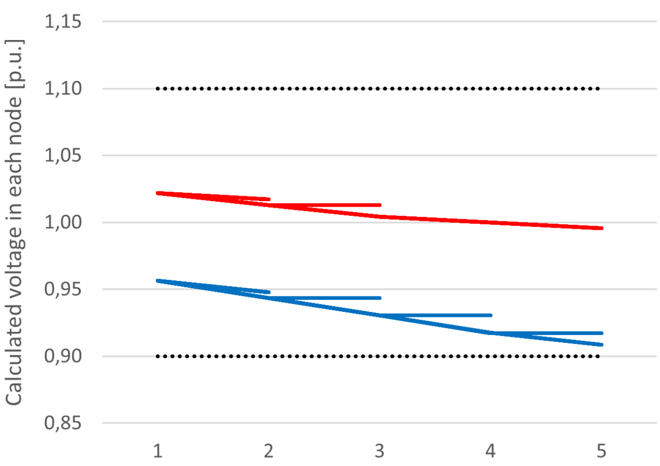


Figure 3.11: Voltage drop for circuit 3 in summer time (red) and winter time (blue) without PV systems.

### 3.2.5 Study case 4

Figure 3.12 shows the PowerFactory model of study case 4 with ten customers, and the distribution transformer is 315 *kVA*.

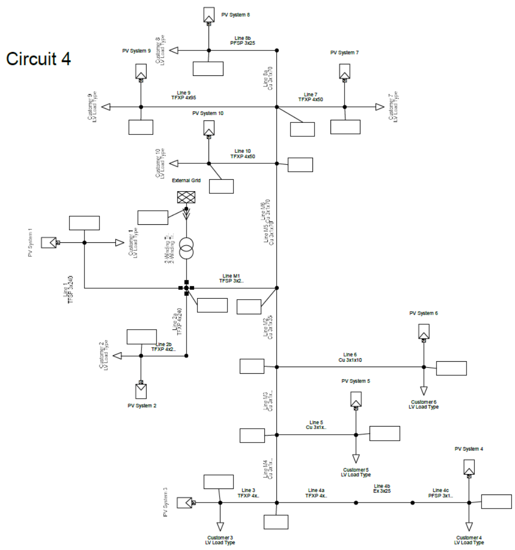


Figure 3.12: Substation circuit 4 represented in PowerFactory.

The voltage drop for circuit 4 is shown in figure 3.13. The summer load was significantly lower than the winter load, resulting in the red summer load graph having so little voltage drop. This circuit has one customer with a low $I_{sc2min}$-value of 293 A and a voltage drop of 18 V or almost 0,08 pu. The customer with the strongest grid has a $I_{sc2min}$ of 10 214 A.

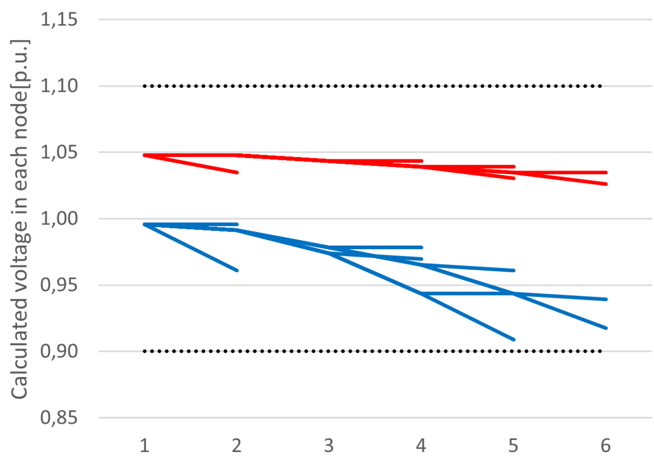


Figure 3.13: Voltage drop for circuit 4 in summer time (red) and winter time (blue) without PV systems.

## 3.3 PowerFactory simulations

### 3.3.1 Short circuit current calculations

The models from study cases 1 to 4 use short circuit analysis of Trimble and PowerFactory. The short circuit result can compare the circuits and ensure the correct modeling of the PowerFactory circuits. This will ensure that the external grid, transformer, lines, and cables are comparable from Trimble to PowerFactory. The short circuit current is later used to describe the impact on the grid as load and production vary.

### 3.3.2 Load flow analysis

The load flow analysis of PowerFactory can simulate the voltage variations and thermal loading of components. The thresholds of the grid are found by using summer load and subjecting the circuit to increasing PV system until surpassing the limitation. The low voltage level is set by simulating winter load with no PV and then using a tap changer on the distribution transformer to tap down so that the customers are closest to possible regulations' lower limit without breaking the limit. This voltage level shows the maximum potential in PV capacity concerning the voltage bandwidth of the circuit.

The measured loads are processed to find two outer limit scenarios. Both scenarios are middle of the day as the PV system produces the most. The first case is the winter load, where the load is on a cold winter day where the load is highest. The second case is a warm summer day with low load consumption. High load corresponds to low voltage, and low load corresponds to high voltage. The PowerFactory models calculate the voltage for each busbar.

### 3.3.3 Harmonic load flow

The models will contribute to two types of harmonic distortion for harmonic load flow. The first is background distortion in the external grid. The grid model uses measured harmonic voltage values to set a 1,1 % THD default. The second contribution is by inserting a harmonic current spectrum in the PV system as described in 3.2. The study cases use the harmonic current spectrum from Patsalides' report with the highest irradiates for a 16 $kW_p$ PV system [22]. Harmonic distortion from the highest irradiation is the case when the harmonic current spectrum is lowest. However, because of the power output from PV, it is the case with the highest harmonic voltages distortion.

# 4 Simulation results

In section 3.2 the study cases were defined without any PV systems. In section 3.3 the PV systems production was defined, and the different simulation methods were described.

This chapter uses the defined study cases and PV system to simulate the different thresholds in the grid for the thermal load, voltage variations, and THD. Simulations will present and use four different scenarios to better understand the impact from PV systems.

## 4.1 Short circuit current results

Table 4.1 shows an overview of customers' minimum short circuit current $I_{sc2min}$ value. The table categorizes the strength of the grid for different circuits presented in chapter 3 as study cases 1 to 4. These circuits are not supposed to represent the general grid but weaker grids, typically found in rural areas. Appendix D show all the results from the short circuit calculations. The results are shown in appendix D.

Table 4.1: An overview of the short circuit value $I_{sc2min}$ of the circuits in study case 1 to 4.

| | <=199 | 200-399 | 400-599 | 600-799 | 800-999 | 1000-1199 | >=1200 |
|---|---|---|---|---|---|---|---|
| Circuit 1 | 1 | 1 | 2 | 1 | 0 | 1 | 0 |
| Circuit 2 | 0 | 3 | 3 | 1 | 0 | 0 | 3 |
| Circuit 3 | 0 | 0 | 1 | 1 | 0 | 2 | 2 |
| Circuit 4 | 0 | 1 | 1 | 1 | 0 | 1 | 6 |

## 4.2 Thermal load

The load flow analysis focuses on three parts regarding thermal load. The first part is the cable or line connecting the customer to the grid, the second part is the feeding lines of the circuit, and the last part is the distribution transformers in the circuit. As seen in table 4.2 the connection cable of the customer does not reach thermal overload, even with very high production.

Table 4.2: Thermal load of most loaded end-customer cable with 100 % PV penetration of 25 $kW_p$ each during summer load.

| | Circuit 1 [%] | Circuit 2 [%] | Circuit 3 [%] | Circuit 4 [%] |
|---|---|---|---|---|
| End-customer cable | 48,9 | 61,2 | 43,3 | 71,2 |

The simulation results in table 4.2 shows that even with a full PV penetration, each with a 25 $kW_p$ production, and with a minimal load situation, the highest thermal load of a customer connection cable is 71,2 %.

Table 4.3: The feeding cable's thermal load with 100 % PV penetration of 25 $kW_p$ each customer during summer load.

| | Circuit 1 [%] | Circuit 2 [%] | Circuit 3 [%] | Circuit 4 [%] |
|---|---|---|---|---|
| Feeding line 1 | 77,4 | 59,1 | 46,6 | 94,9 |
| Feeding line 2 | 38,9 | 48,5 | 33,1 | 119 |
| Feeding line 3 | | 28,4 | 24,1 | 86,4 |
| Feeding line 4 | | 98,6 | | 88,1 |
| Feeding line 5 | | 79 | | 73 |
| Feeding line 6 | | 58,1 | | 54,6 |

The simulation results in table 4.3 shows the thermal load for all feeding cables at 100 % PV penetration and 25 $kW_p$ production. The red number in feeding line 2 in circuit 4 means that the cable is thermally overloaded when all customers produce energy with a 25 $kW_p$ PV system. Notice that this is thermal overload with reversed power flow.

Table 4.4: The transformer's thermal load in the circuit with 100 % PV penetration with different installed rated power of PV systems each during summer load.

| Transformer | Circuit 1 [%] | Circuit 2 [%] | Circuit 3 [%] | Circuit 4 [%] |
|---|---|---|---|---|
| 0 $kW_p$ | 43,5 | 29,5 | 59,3 | 10,7 |
| 5 $kW_p$ | 20,4 | 18,2 | 25,3 | 7,8 |
| 10 $kW_p$ | 27 | 71,7 | 70,6 | 22,9 |
| 15 $kW_p$ | 50,4 | 115,6 | 125,4 | 38,3 |
| 20 $kW_p$ | 75,1 | 157,7 | 179,4 | 53,3 |
| 25 $kW_p$ | 99,4 | 198,1 | 232,1 | 67,9 |

Table 4.4 shows the loading of transformer in [%] at 100 % PV penetration with different PV sizes. Red numbers mean that the transformer is thermally overloaded. In circuits 1, 2, and 3, the transformers reach thermal overload before the cables and lines in the same circuits.

## 4.3 Voltage variations

Figure 4.1 shows the voltage drop for circuits 1, 2, 3, and 4. The red lines and blue lines are voltage drops for respective circuits during summer load and winter load. There are no PV systems producing power during winter load, while during summer load, there is a 100 % PV penetration, and all PV systems produce equally and increases until a customer reaches the upper voltage limit of 10 %.

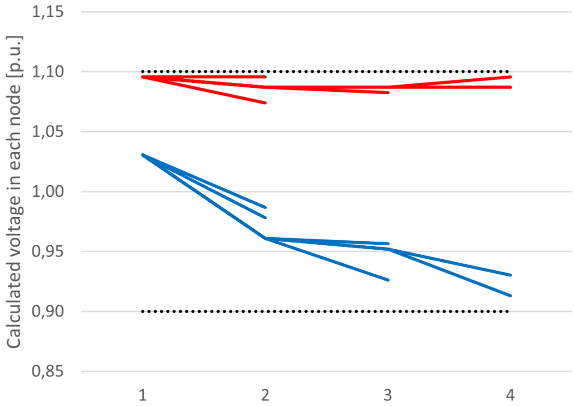


(a) Circuit 1 with the highest PV capacity installed 3,2 $kW_p$.

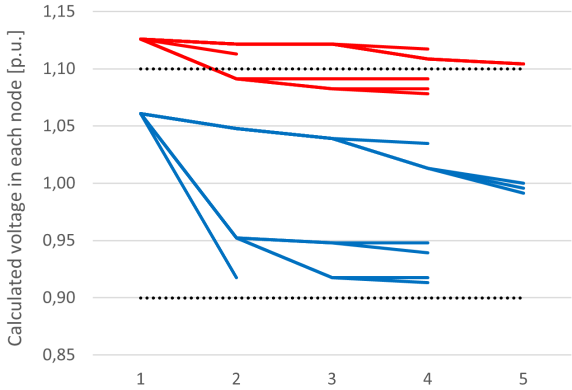


(b) Circuit 2 with no PV systems, as there are no PV capacity.

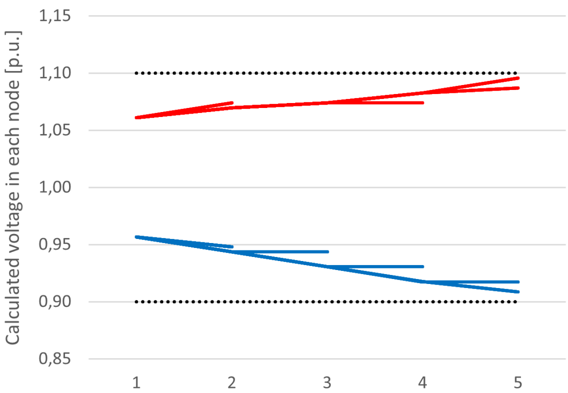


(c) Circuit 3 with the highest PV capacity installed 15,8 $kW_p$.

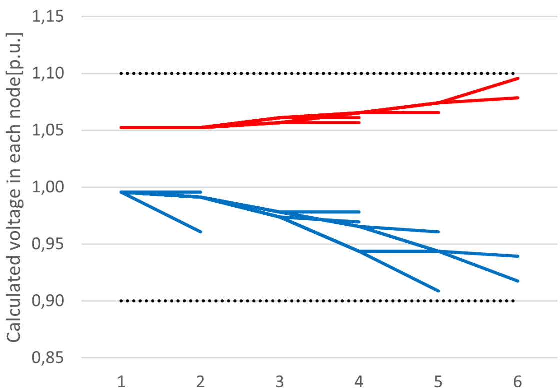


(d) Circuit 4 with the highest PV capacity installed 8,4 $kW_p$.

Figure 4.1: The voltage drop in wintertime (blue lines) and voltage rise during summertime with maximum PV capacity installed (red lines).

Circuit 1 has a production of 3,2 $kW_p$ per customer before a customer reaches the upper voltage limit. As shown in section 3.2.3 circuit 2 was unable to handle the existing load and can therefore not support any PV system. Circuit 3 and 4 can handle respectively 15,8 $kW_p$ and 8,4 $kW_p$, regarding the voltage variation.

### 4.3.1 Variations in high voltage grid

Table 4.5 shows the impact on PV capacity from different percentage variations. Circuit 1 has a capacity for PV systems with up to 5 % variations in the high voltage grid. Circuit 2 has a capacity for PV systems up to 2 %. The simulations will use 4 % from here on. Figure 4.2 displays how the PV capacity shifts linearly as the variations changes.

Table 4.5: The highest PV capacity [$kW_p$] in circuits 1 to 4 with 100 % PV penetration for different percentage variations in a high voltage grid.

| | 0 % | 1 % | 2 % | 3 % | 4 % | 5 % | 6 % | 7 % |
|---|---|---|---|---|---|---|---|---|
| Circuit 1 | 6,5 | 6 | 5,5 | 3,8 | 2,8 | 1 | | |
| Circuit 2 | 3,3 | 2 | | | | | | |
| Circuit 3 | 24 | 21 | 19 | 17,5 | 15,8 | 14,1 | 12,3 | 10,6 |
| Circuit 4 | 13,2 | 12 | 10,8 | 9,6 | 8,4 | 7,2 | 6 | 4,8 |

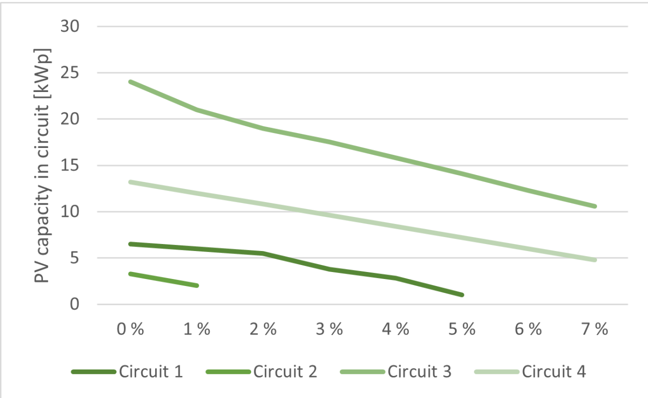


Figure 4.2: The highest PV capacity [$kW_p$] in circuits 1 to 4 with 100 % PV penetration for different percentage variations in a high voltage grid.

## 4.4 Harmonic distortion from prosumers

Figure 4.3 shows all four circuits simulated with 100 % PV penetration, where all PV systems produces 25 $kW_p$ electricity. Simulations for THD indicates that higher load increases the impact from THD, therefore, simulation uses winter load for simulating THD. The highest calculated THD is 6,5 % with circuit 2. The simulations do not surpass the regulation limit of 8 %.

The maximum PV capacity at 100 % PV penetration is shown in table 4.6. The limiting customer is the first to surpass the regulation limit of 8 % limit. In circuit 2 and 3, the customer who limit PV capacity regarding THD, is the same customers with least

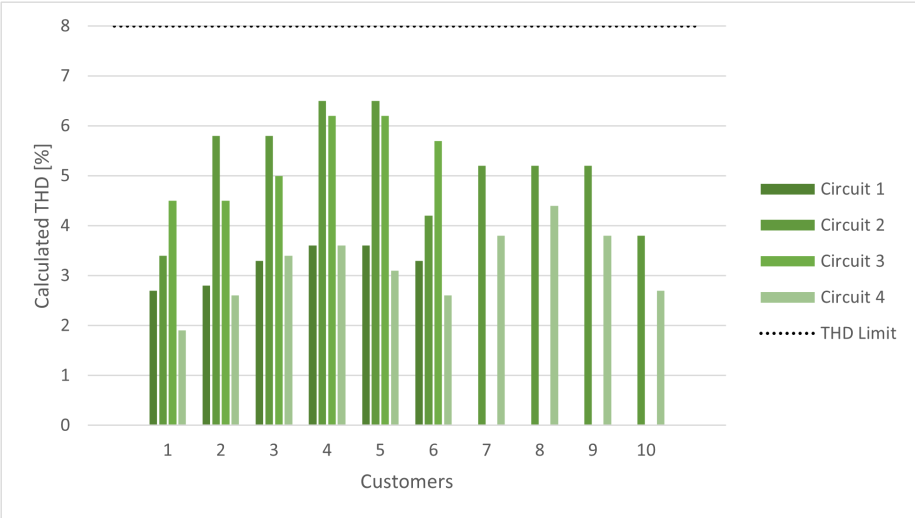


Figure 4.3: The calculated THD for each customer at 100 % PV penetration as installed power from PV is 25 $kW_p$ per customer.

minimum short circuit currents in their circuits. In contrast to circuits 1 and 4, the customers who limits the PV capacity regarding THD are not the same as those with the least minimum short circuit current.

Table 4.6: The maximum installed PV capacity at 100 % PV penetration regarding the regulations' THD limit of 8 %.

| | THD | Limiting customer |
|---|---|---|
| Circuit 1 | 105 $kW_p$ | Customer 4 |
| Circuit 2 | 40 $kW_p$ | Customer 4 and 5 |
| Circuit 3 | 33 $kW_p$ | Customer 4 and 5 |
| Circuit 4 | 65 $kW_p$ | Customer 8 |

## 4.5 Prosumers close versus far from substation

In figure 4.4 each color is a case with 50 % PV penetration, which in this case means three customers with PV systems and three customers without it. The yellow line shows the case where all the PV systems are nearby the substation. In contrast, the green line shows the case where all the PV systems are far from the substation. The case with close PV systems could handle 32 $kW_p$ while the PV systems far away from the substation could only handle 19 $kW_p$.

Table 4.7 shows results from simulating the cases of PV systems far versus close to the substation. Each case increases the PV system until the case reaches the upper voltage

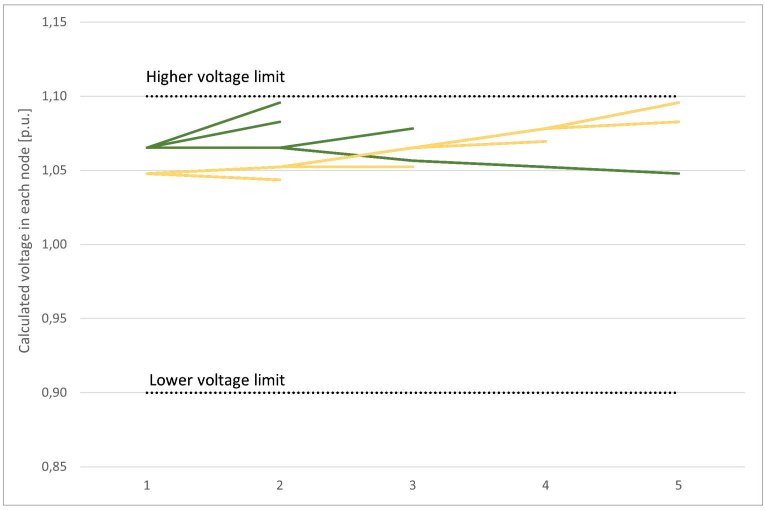


Figure 4.4: Voltage drop for 50 % PV penetration in circuit 3. Green is PV system placed close to substation, yellow is PV system placed far from substation.

limit or the thermal overload. Notice that in circuit 3, the limiting factor is the transformer when the PV systems are close to the substation. In circuit 4, the customers' connection cable for customer 6 limits the PV capacity when the PV systems are close to the substation.

Table 4.7: The highest PV capacity for circuits 1 to 4 for 50 % PV penetration regarding PV system close versus far from the substation.

| | Close | Far |
|---|---|---|
| Circuit 1 | 10,6 $kW_p$ Voltage | 6,2 $kW_p$ Voltage |
| Circuit 2 | - | - |
| Circuit 3 | 25,4 $kW_p$ Thermal transformer | 20,8 $kW_p$ Voltage |
| Circuit 4 | 35,3 $kW_p$ Thermal connection cable | 9 $kW_p$ Voltage |

## 4.6 Farms as prosumers

Many farms make challenging cases in the distribution grid. They are often in rural areas with a weaker grid, and they are often customers with high consumption and have a bigger main switch than most other customers in rural areas. Farms tends to have buildings with extensive roof areas which are suitable for many PV panels.

In circuit 1, customer 4 is an average size farm. As customer 4 produces 19,7 $kW_p$ and all other customers produce no power, the voltage of customer 4 reaches 252 V. When all other customers produce 5 $kW_p$, then customer 4 is only able to produce 7 $kW_p$ before the voltage of the neighbor customer 5 reaches 252 V.

As earlier mentioned, circuit 2 has no PV capacity with the existing grid.

In circuit 3, customer 1 is an average size farm. As customer 1 produces 77,5 $kW_p$ and all other customers produce no power, the thermal load of the transformer limits the circuit. If all other customers produce 5 $kW_p$, then customer 1 can only produce 51 $kW_p$ before thermally overloading the transformer.

In circuit 4, customer 1 is an above-average size farm. As Customer 1 produces 348 $kW_p$, and all other customers do not produce any, the thermal load in both transformer and connection cable limits the PV capacity in the circuit. As all other customer produces 5 $kW_p$, and customer 1 produces 300 $kW_p$, the thermal limit of the transformer limits the PV capacity.

The THD for all simulations is between 1 and 4 % and is not close to limiting the PV capacity.

## 4.7 Simulation of countermeasures

Earlier in this chapter, four circuits were simulated to find the general PV capacity for all customers in a circuit. In the section 4.7 the study case will upgrade the circuits. The first case will change the transformer, and the second case will reinforce 50 % of the feeding lines in the circuits. The simulations will focus on how the countermeasure will impact the PV capacity concerning THD, thermal overload, and voltage variation.

### 4.7.1 Changing transformers

The most common reason to change a distribution transformer is due to an increase in load situation. Distribution transformers have standardized impedance. The impedance is given as a percentage value of the rated power of the transformer. If two transformers with equal impedance but different rated power, higher rated power means lower impedance at the same load [51]. The grid impedance will decrease when upgrading the substation with a new transformer, and the short circuit current will increase. In table 4.8 shows the increasing of $I_{sc2min}$ when upgrading the transformer one size. Changing transformers have highest impact on customers with the highest short circuit currents. Customers close to the substation usually have high short circuit currents, strongly affected by the distribution transformer. In contrast, cables and lines strongly define the short circuit current for customers far out in the grid. See simulations results from load flow analysis in section 4.8.

Table 4.8: The change in the least short circuit current $I_{sc2min}$ [A] when upgrading the distribution transformer.

| Circuit 1 | | Circuit 2 | | Circuit 3 | | Circuit 4 | |
|---|---|---|---|---|---|---|---|
| 100 *kVA* | 200 *kVA* | 100 *kVA* | 200 *kVA* | 50 *kVA* | 100 *kVA* | 315 *kVA* | 500 *kVA* |
| 387 | 397 | 1346 | 1518 | 1430 | 2003 | 10214 | 14116 |
| 1115 | 1234 | 384 | 397 | 1033 | 1281 | 1003 | 1022 |
| 529 | 550 | 354 | 365 | 1297 | 1760 | 692 | 698 |
| 438 | 452 | 262 | 268 | 704 | 821 | 293 | 294 |
| 184 | 186 | 293 | 301 | 530 | 591 | 1413 | 1444 |
| 793 | 844 | 1456 | 1697 | 983 | 1229 | 2114 | 2186 |
| | | 695 | 742 | | | 1452 | 1497 |
| | | 467 | 486 | | | 506 | 510 |
| | | 506 | 529 | | | 1520 | 1571 |
| | | 1268 | 1426 | | | 2728 | 2869 |

### 4.7.2 Upgrading cables and lines in grid

Upgrading the grid means either changing the lines or changing the topology by adding more cables or lines. In this case, all circuits change 50 % of the feeding lines closest to the substation to the cable TFXP 4x240 Al. Table 4.9 shows that the upgrade increases the $I_{sc2min}$ value for all customers connected to the substation through the feeding cables.

Table 4.9: The change in the least short circuit current $I_{sc2min}$ [A] when upgrading the grid by changing 50 % of feeding lines in each circuit.

| Circuit 1 | | Circuit 2 | | Circuit 3 | | Circuit 4 | |
|---|---|---|---|---|---|---|---|
| | Upgrade | | Upgrade | | Upgrade | | Upgrade |
| 387 | 387 | 1346 | 1346 | 1430 | 1430 | 10214 | 10214 |
| 1115 | 1115 | 384 | 859 | 1033 | 1033 | 1003 | 1003 |
| 529 | 698 | 354 | 726 | 1297 | 1461 | 692 | 764 |
| 438 | 545 | 262 | 421 | 704 | 794 | 293 | 305 |
| 184 | 201 | 293 | 507 | 530 | 575 | 1413 | 1751 |
| 793 | 1214 | 1456 | 1960 | 983 | 1171 | 2114 | 2970 |
| | | 695 | 792 | | | 1452 | 1652 |
| | | 467 | 509 | | | 506 | 527 |
| | | 506 | 556 | | | 1520 | 1741 |
| | | 1268 | 1402 | | | 2728 | 3511 |

Notice that the length of the cables and lines is not changed. The upgrade of circuit 1 changes the feeding line M1. The upgrade of circuit 2 changes feeding lines M1, M4, and M5. The upgrade in circuit 3 divides the feeding line M2 in two, changing the feeding line

M1 and half of the feeding line M2. The upgrade in circuit 4 changes the feeding lines M1, M2, and M5. With new feeding lines, a new calibration of the distribution transformers tap changer is done. The tap changer resets the voltage level to review the maximum PV capacity.

## 4.8 Summarizing and comparing simulation results

Table 4.10 shows the PV capacity for circuits 1 to 4 regarding the different limiting parameters; THD, thermal loading in cables, thermal loading in transformer, and voltage limitation.

Circuit 1 was limited by voltage variation, being able to connect 3,2 $kW_p$ for all customers. The thermal load was not a problem before 25 $kW_p$, at which the transformer reached a thermal load of 99,4 %.

During winter, the voltage drop for Circuit 2 was so high, that the circuit is unable to ensure voltage inside the limits of Norwegian regulation. There was no PV capacity in this circuit. Therefore, looking for opportunities for upgrading grids is necessary. Considering THD and thermal loading, the PV capacity limits are better.

Circuit 3 has a capacity of 12,2 $kW_p$, at which the transformer would reach thermal load right under 100 %. The voltage limits the PV capacity to 15,8 $kW_p$.

Circuit 4 was limited by voltage variation, as PV systems reached a production of 8,4 $kW_p$.

Table 4.10: The highest PV capacity for circuits 1 to 4 at 100 % PV penetration for different limiting factors.

| | THD | Line | Transformer | Voltage | Limiting parameter |
|---|---|---|---|---|---|
| Circuit 1 | 105 $kW_p$ | 32 $kW_p$ | 25 $kW_p$ | 3,2 $kW_p$ | Voltage variation |
| Circuit 2 | 40 $kW_p$ | 27,5 $kW_p$ | 13,8 $kW_p$ | - | Voltage variation |
| Circuit 3 | 33 $kW_p$ | 49,9 $kW_p$ | 12,2 $kW_p$ | 15,8 $kW_p$ | Transformer |
| Circuit 4 | 65 $kW_p$ | 21 $kW_p$ | 35,7 $kW_p$ | 8,4 $kW_p$ | Voltage variation |

Comparing table 4.10 with table 4.11. Results indicate that increasing transformer size will decrease the amount of THD. The line capacity decreases because changing the transformer allows tapping the substation voltage even lower to allow a higher capacity for PV systems. According to Ohm's law, as the voltage is slightly lower, the current will increase, causing thermal overload sooner. Regarding the transformer, upgrading the transformer will increase the transformer's capacity in the circuit.

Comparing table 4.12 with table 4.10. The results indicate that increasing the strength of the cables in the grid will increase the impact of THD. The line capacity increases

Table 4.11: The PV capacity in circuits 1 to 4 at 100 % PV penetration that surpasses the limits when transformer is upgraded.

| | THD | Line | Transformer | Voltage | Limiting factor |
|---|---|---|---|---|---|
| Circuit 1 200 $kVA$ | 190 $kW_p$ | 31 $kW_p$ | 46 $kW_p$ | 5,1 $kW_p$ | Voltage |
| Circuit 2 200 $kVA$ | 50 $kW_p$ | 25,7 $kW_p$ | 25,7 $kW_p$ | - | Voltage |
| Circuit 3 100 $kVA$ | 49,5 $kW_p$ | 48 $kW_p$ | 20,8 $kW_p$ | 19 $kW_p$ | Voltage |
| Circuit 4 500 $kVA$ | 80 $kW_p$ | 21 $kW_p$ | 57 $kW_p$ | 8,4 $kW_p$ | Voltage |

as the upgrade change the most loaded feeding lines. The voltage variation increases significantly for circuit 2, as an upgrade in the grid reduces the voltage drop in winter load significantly, giving the circuit potential PV capacity. The voltage limit significantly increases the PV capacity in circuits 1 and 2, as they were worse than circuits 3 and 4 before the upgrade. Therefore, the upgrade is more significant in circuits 1 and 2. Figure 2.4 shows that the voltage drop in feeding lines for circuits 1 and 2 is bigger than for circuits 3 and 4.

Table 4.12: The PV capacity in circuits 1 to 4 at 100 % PV penetration that surpasses the limits when 50 % feeding lines are upgraded.

| | THD | Line | Transformer | Voltage | Limiting factor |
|---|---|---|---|---|---|
| Circuit 1 | 82 $kW_p$ | 51,5 $kW_p$ | 24 $kW_p$ | 5,7 $kW_p$ | Voltage |
| Circuit 2 | 36 $kW_p$ | 42,5 $kW_p$ | 13 $kW_p$ | 9,1 $kW_p$ | Voltage |
| Circuit 3 | 36 $kW_p$ | 59,8 $kW_p$ | 12,2 $kW_p$ | 16,3 $kW_p$ | Transformer |
| Circuit 4 | 72 $kW_p$ | 28,3 $kW_p$ | 35,8 $kW_p$ | 9,1 $kW_p$ | Voltage |

Simulation in PowerFactory finds the highest THD with evenly distributed PV systems in the places where the short circuit current is small. In cases with multiple and nearby neighbors producing THD, the simulations find the highest THD in the connection point between these prosumers.

Results from the far versus close case show that PV capacity is better the closer the PV system is to the substation. For circuits 1, 3, and 4, results show that farms' grid connections generally have a good PV capacity, and circuit 4 has the most capacity, up to 345 $kW_p$.

In figure 4.5 the light green line is the maximum PV capacity at different $I_{sc2min}$ values, simulated from three different cases at each circuit. As earlier mentioned in this chapter, the three different cases are; normal situations, with transformer upgrade and with the upgrade of feeding lines. The darker green line is a calculated PV capacity from the equation given in the figure 4.5. Where $\Delta U$ is voltage drop from substation voltage at summer load before installing PV system to the customer. The figure does not include study case 2 before the upgrade and study case 2 after upgrading the transformer, as they had no PV capacity in simulation or calculation.

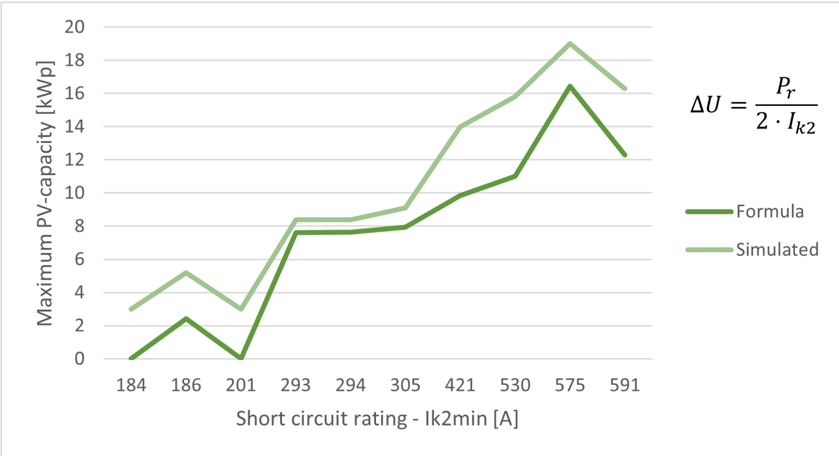


Figure 4.5: Calculated and simulated maximum PV capacity.

# 5 Discussion

In chapter 3 the circuits with loads and PV systems were defined. In chapter 4, the circuits were subjected to increasing PV systems to find the grid threshold in different situations.

The discussion chapter is divided into four parts. The first part is the uncertainties in models. The second part uses the results to describe the more general PV capacity in circuits. The third part will discuss the situation of Lede, and the last part is a short discussion of one-phase inverters.

## 5.1 Uncertainties in models

This section comments on the choices made in chapter 3 and how they impact the results. A model will have some deviation from the system, and understanding the deviation will form a basis for interpreting simulation results into realistic cases.

### 5.1.1 The cables, lines and external grid

The data quality between PowerFactory and Trimble is considered good, as the comparing of short circuit currents between Trimble and PowerFactory for all customers, shows approximately equal results. It is essential to be aware that Trimble does have some minor deviation regarding lengths and, in some cases, actual cable types between the actual grid and the model. This deviation is assumed to have minimal significance for case studies.

### 5.1.2 Voltage

The voltage set in the substation will usually be around 240 V. In the simulations, the substation voltage was set as low as possible to review the potential for PV capacity in the grid. If the objective is to check the grid's capacity as the grid is today, then the results will be too optimistic. Assuming that there is free capacity in the voltage bandwidth, the DSO would adjust the tap changer to avoid unnecessary grid investments. Then the results show the actual PV capacity potential without any significant measures to the grid.

Because of uncertainty in actual values, the variation in the high voltage grid was set to 4 %. The impacts from different variations were conducted in subsection 4.3.1, which shows that variations in the high voltage grid have a high impact on the PV capacity in the circuits.

### 5.1.3 Load

There have been used two types of values for load; winter and summer load. Both are measured as an average of over an hour. The winter load used the highest measured value for all cases in February, and the summer load was the average load on a hot summer day around noon. Two factors are neglected regarding load. The first is that AMS measurements are measured averagely over one hour. The load can be higher and lower inside the measured hour. The winter load, the maximum measured load, could be higher. The second factor is neglecting the diversity factor because not all households use maximum consumption simultaneously, reducing the total load in winter for all circuits. Considering these two factors and that the used measured winter load has only been recorded one time, the results will be conservative. At last, the load profile assumes symmetrical loads. If there is a variation in load distribution between phases, the results might be optimistic.

### 5.1.4 PV system

The simulations of PV systems in this report use no diversity factor. No diversity factor means that all roof orientation and angles are the same for all PV systems in a circuit. If all customers in a circuit had a PV system, it would be unlikely that all customers would have the same roof orientation and angles. Therefore, it is likely to assume some diversity factor, and the results of this report are conservative, as simulated PV capacity must be smaller than actual PV capacity.

In terms of rated power for a PV system, the simulations use the rated power peak value as producing value. In a more realistic case, there would be a performance ratio, reducing the efficiency of PV systems. The performance ratio was set to 100 % in the simulations, but as mentioned in section 2.2.1, the performance ratio will often be around 80 % to 90 %.

At last, the power factor of the PV system was simulated with a cos phi of 1. PV systems can offer some degree of reactive compensation, which would slightly decrease the load and voltage. These four aspects of the simulation state that the model for PV systems is very conservative.

### 5.1.5 THD

The THD from the overlying grid originates from using measured data for THD, 3rd, 5th and 7th order harmonic voltage. The simulations do not focus on individual harmonic distortion, making it easier to compare the limitation of PV capacity between harmonic distortion, thermal load, and voltage variation. All PV systems in this report use the same harmonic current distortion spectrum. The harmonic current spectrum is found in a report that only shows the spectrum for one phase [22]. Therefore, the spectrum assumes equal values for the other phases, but the phase angles shift 120 degrees. The harmonic current spectrum is from a 16 $kW_p$ PV system, and it is unknown how the spectrum changes as PV system size increases. It is unsure if the simulations for when all PV systems have an equal harmonic spectrum, make the results conservative or optimistic.

## 5.2 PV capacity in rural areas

In this project, four study cases represent distribution grids in rural areas in Norway. They have few customers, long lines and cables, and the distribution transformers have low-rated power. In three of four circuits, the voltage variation limits the PV capacity of the circuits. In the last circuit, the thermal overload of a transformer limits the PV capacity.

Table 5.1 shows the simulation results, and the simulations conclude that the PV capacity for older and rural distribution grids is between 0 to 12 $kW_p$ at 100 % PV penetration. PQA states in their report a general PV capacity of 0 to 8 $kW_p$ of rural distribution grid. The PV capacity is higher closer to the substation, and farms typically have a stronger connection to the substation and better capacity than regular households.

Table 5.1: The highest PV capacity for circuits 1 to 4 at 100 % PV penetration for different limiting factors, 4 % high voltage variation is included.

| | THD | Line | Transformer | Voltage | Limiting parameter |
|---|---|---|---|---|---|
| Circuit 1 | 105 $kW_p$ | 32 $kW_p$ | 25 $kW_p$ | 3,2 $kW_p$ | Voltage variation |
| Circuit 2 | 40 $kW_p$ | 27,5 $kW_p$ | 13,8 $kW_p$ | - | Voltage variation |
| Circuit 3 | 33 $kW_p$ | 49,9 $kW_p$ | 12,2 $kW_p$ | 15,5 $kW_p$ | Transformer |
| Circuit 4 | 65 $kW_p$ | 21 $kW_p$ | 35,7 $kW_p$ | 8,4 $kW_p$ | Voltage variation |

The report conducts two cases to increase the capacity, changing the transformer one size and changing 50 % of feeding lines to a stronger cable were considered. Changing the transformers increased the PV capacity regarding voltage variation with an average of 1,3 $kW_p$. Changing the feeding cable increased the PV capacity regarding voltage variation with an average of 2,5 $kW_p$. In the last case, the transformer size limited the PV capacity of two circuits.

$$P_r[kW_p] = (252[V] - U_{substation}[V]) \cdot 2 \cdot I_{sc2min}[kA] \cdot 1.3 \quad (5.1)$$

The equation 5.1 rewrites the equation shown in figure 4.5 to predict the maximum PV capacity of a circuit. The equation for maximum PV capacity is defined in equation 5.1 where $P_r$ is the circuits' PV capacity for one customer, $252[V]$ is the voltage limit, $U_{substation}$ is the substation voltage during the summertime, and $I_{sc2min}$ is the lowest minimum short circuit current in the circuit. Figure 5.1 shows the equation in use for different substation voltages. For example, a circuit with a substation voltage of 245 V and the customer with the lowest minimum short circuit current of 800 A would have a PV capacity of 14,56 $kW_p$. Note that this PV capacity is only valid for voltage variation.

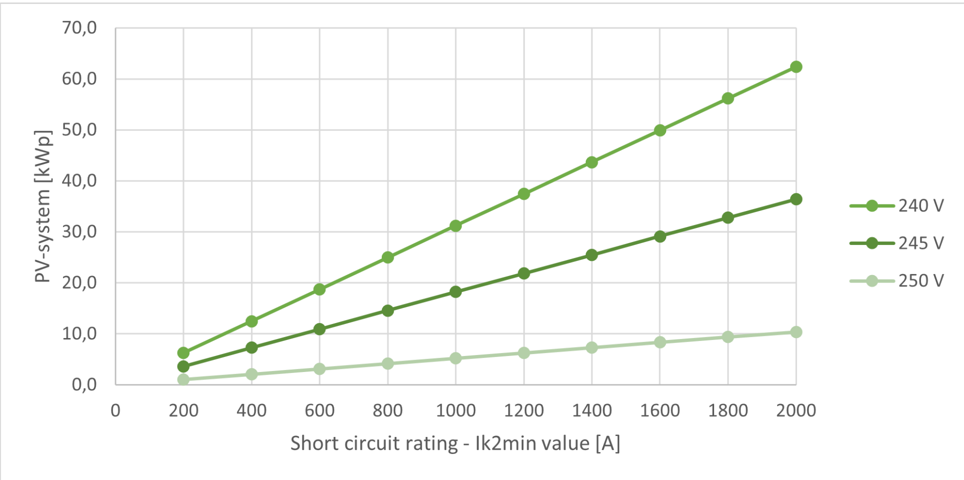


Figure 5.1: General limit for PV system in circuit based on lowest minimum short circuit current in circuit and different calculated substation voltage.

## 5.3 Future trends of prosumers

The amount and size of PV systems have increased in the Lede AS' grid area. Table 5.2 shows that the average size of a PV system is almost 13,4 $kW_p$. The data from Lede is limited, as it only shows data from 2017, and the data pattern is recognizable to the level that it is increasing. Supported with data from NVE and IEA, it is safe to assume a stable, increasing pattern.

Table 5.3 shows the lowest minimum short circuit currents for every circuit operated by Lede AS. Circuits 1, 2, and 4 can represent 714 of Lede's substation circuits with the lowest minimum short circuit current $I_{sc2min}$ less than 300 A. These circuits have according to results a PV capacity of between 0 and 8,4 $kW_p$ per customer. As the average PV system

Table 5.2: Total installed PV system for Lede AS operating area (installations under 100 $kW$).

| Year | Number | Total installed power [$kW_p$] | Average installed power [$kW_p$] |
|---|---|---|---|
| 2017 | 52 | 471.28 | 9.06 |
| 2018 | 103 | 1017.37 | 9.88 |
| 2019 | 233 | 2087.90 | 8.96 |
| 2020 | 234 | 3457.87 | 14.78 |
| 2021 | 215 | 2876.4 | 13.385 |

was 13,4 $kW_p$ in 2021 and 14,78 $kW_p$ in 2020, the circuits with a low short circuit current cannot install the average PV installation without reducing the PV capacity for other customers in the same circuit.

Table 5.3: An overview of the least minimum short circuit current $I_{sc2min}$ for every substation circuits in Lede AS operating area.

| Least minimum short circuit current $I_{sc2min}$ in a substation circuit. | | | | | | | |
|---|---|---|---|---|---|---|---|
| <=199 | 200-399 | 400-599 | 600-799 | 800-999 | 1000-1199 | 1200-1399 | >=1400 |
| 173 | 1311 | 1293 | 1105 | 770 | 465 | 289 | 2077 |

## 5.4 One-phase inverter

Earlier, when the inverter technology was immature and expensive, most inverters for PV systems for households were one-phase inverters. The one-phase inverter is an equipment that can cause voltage imbalance. Therefore it was important for DSO to demand three-phase inverters for PV systems rated for 16 $A$ or more. It is unsure if these older installations were responsible for any grid upgrades that could be avoided by using three-phase inverters.

# 6 Conclusion and further work

As the report from PQA AS concludes that the PV capacity is very good for urban and industrial areas, this thesis has focused on the rural area with older circuits [6]. Equation 6.1 presents a general threshold for PV capacity in a circuit, in respect to voltage variation, the equation is derived as:

$$P_r[kW_p] = (252[V] - U_{substation}[V]) \cdot 2 \cdot I_{sc2min}[kA] \cdot 1.3 \tag{6.1}$$

Where $P_r$ is the PV capacity for all customers in the same circuit that can be installed without surpassing the voltage limit in $[kWp]$. 252 $[V]$ is the voltage limit according to FOL [10]. $U_{substation}$ is the substation voltage at summer load in $[V]$. $I_{sc2min}$ is the least minimum short circuit current in the circuit in $[A]$. From equation 6.1 we derive the figure 6.1. The figure shows general PV capacity regarding voltage variation for three different values of substation voltage, and the x-axis is the least minimum short circuit current in a circuit.

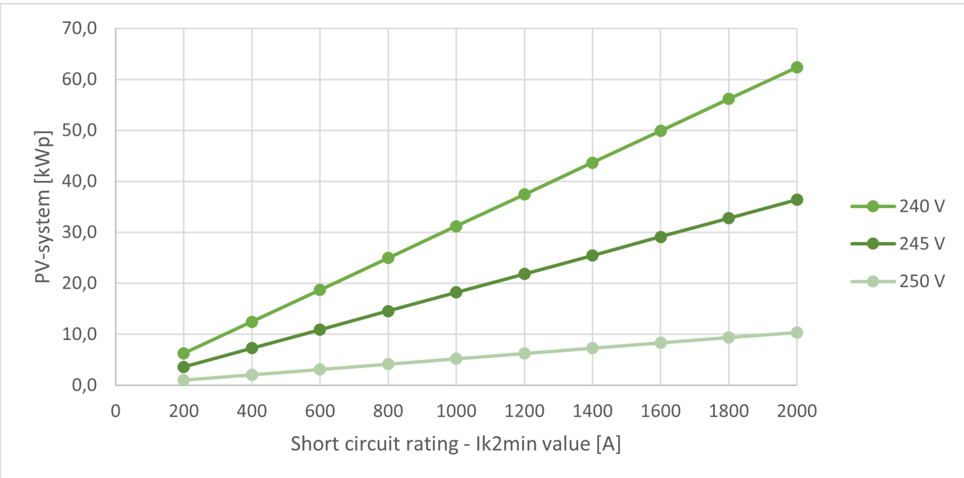


Figure 6.1: General PV capacity regarding voltage variation in a circuit based on the least short circuit current in the circuit and different calculated substation voltage.

If a planned PV system is larger than $P_r$, the grid manager can upgrade the grid or consider accepting the PV system at the risk of reducing the PV capacity for all other customers in the circuit. As earlier mentioned, the PV capacity is greater, closer to the substation. Customers with cables with higher capacity as connection cables, for instance, farms, usually have better PV capacity than the other customers.

If the planned PV system is smaller than $P_r$, it is essential to look at the thermal overloading of cables and transformers. The load situation in the circuit should not surpass any thermal limit during the wintertime, and the production situation for PV systems should not surpass any thermal limit during the summertime.

Results from the simulation suggest that the THD will not limit the PV capacity for households and farms in rural areas.

Simulations for the three representative cases, circuit 1, 2, and 4, concludes that 714 of Lede's substation circuits with the minimum short circuit current generally have a PV capacity of between 0 and 8,4 $kW_p$ at 100 % PV penetration, which is less than the average installed PV system from 2021 (13,4 $kW_p$). These 714 of Lede's 7172 substation circuits are at a high risk of needing an investing in the grid to increase PV capacity to avoid big voltage variations.

It is important to consider thermal overload as well as voltage variation. Circuit 3 has a higher short circuit current than the other circuits with an $I_{sc2min}$ of 530 A. It is the transformer of this circuit that limits the PV capacity, not the voltage variation.

Upgrading the grid by changing the transformer to increase the PV capacity had little effect. The short circuit current of the customers closest to the substation increased most, rather than those customers limiting the PV capacity with low short circuit currents causing voltage variations. However, for circuits 1 and 3, a transformer change increased the capacity 1-2 $kW_p$. Circuit 2 had no PV capacity, even after the change of transformer.

Upgrading the grid by changing the feeding lines to stronger cables had a better effect of increasing PV capacity by increasing the short circuit currents of the weakest customers, that were connected to the feeding lines. Circuits 1 and 2 increased their PV capacity with 2,5 $kW_p$ and 9,1 $kW_p$ respectively. The impact on PV capacity by changing lines to cables is heavily affected by the amount of feeding lines that is changed and the original lines.

Further work can do similar research for TN network and for urban and industrial areas. Many of the parameters used in this report is neglected or uses a conservative value. For instance the effect total diversity factor and performance ratio for PV systems. The impact from equal and different harmonic spectrums to the THD. The THD impacts for grid with high penetration of power electronics. To ensure correct PV capacity, the variations of high voltage grid should be investigated, and creating statistics for different substations' variations. It would be interesting to simulate and compare newer technology as measures in the grid, for instance, curtailment, reactive compensation, distribution transformer with automatic tap changer, energy storage, and voltage series regulators.

# References


[1] United Nations Climate Change. ‘Key aspects of the paris agreement.’ (), [Online]. Available: https://unfccc.int/process-and-meetings/the-paris-agreement/the-paris-agreement/key-aspects-of-the-paris-agreement (visited on 06/05/2022).

[2] IEA. ‘Solar pv.’ (2021), [Online]. Available: https://www.iea.org/reports/solar-pv (visited on 24/03/2022).

[3] NVE. ‘Solkraft.’ (2021), [Online]. Available: https://www.nve.no/energi/energisystem/solkraft/ (visited on 24/03/2022).

[4] Olje- og energidepartementet, *Forskrift om kraftomsetning og nettjenester*, https://lovdata.no/dokument/SF/forskrift/1999-03-11-301, 1999.

[5] REN AS, ‘Praktisk håndtering av plusskunder,’ 3040, 2020.

[6] M. Lillebo, H. Kirkeby and T. Holm, ‘Prosumenters innvirkning på lavspente distribusjonsnett,’ 2, 2020.

[7] J. Johansson, ‘Optimization of section points locations in electric power distribution systems,’ Mãlardalens högskola, May 2015.

[8] S. Svarte and J. H. Sebergsen, *Energiproduksjon og energidistribusjon*. Gyldendal, 2013, ISBN: 978-82-05-27493-8.

[9] B. K. Perera, P. Ciufo and S. Perera, ‘Point of common coupling (pcc) voltage control of a grid-connected solar photovoltaic (pv) system,’ in *IECON 2013 - 39th Annual Conference of the IEEE Industrial Electronics Society*, 2013, pp. 7475–7480. DOI: 10.1109/IECON.2013.6700377.

[10] Olje- og energidepartementet, *Leveringskvalitetsforskriften*, https://lovdata.no/dokument/SF/forskrift/2004-11-30-1557, 2004.

[11] Skagerak Energi. ‘Nå kommer ams målerne.’ (2017), [Online]. Available: https://www.skageraknytt.no/2017/na-kommer-ams-malerne-article1227-1767.html (visited on 07/05/2022).

[12] NVE. ‘Smarte strømmålere (ams).’ (2015), [Online]. Available: https://lede.no/ams-automatisk-strommaler/category2777.html (visited on 07/05/2022).

[13] Louise Vestergaard-Hansen. ‘Radiokommunikasjon og datasikkerhet i kamstrups strømmålernettverk.’ (), [Online]. Available: https://www.vangenergi.no/media/1089/faq.pdf (visited on 12/05/2022).

[14] A. P. Kenneth and K. Folly, 'Voltage rise issue with high penetration of grid connected pv,' *IFAC Proceedings Volumes*, vol. 47, no. 3, pp. 4959–4966, 2014, 19th IFAC World Congress, ISSN: 1474-6670. DOI: https://doi.org/10.3182/20140824-6-ZA-1003.01989. [Online]. Available: https://www.sciencedirect.com/science/article/pii/S1474667016423839.

[15] S. N. Vikas Khare and P. Baradar, *Ocean Energy Modeling and Simulation With Big Data*. Butterworth-Heinemann, 2020, ISBN: 978-0-12-818904-7.

[16] R. Bauliss and B. J. Hardy, *Transmission and Distribution Electrical Engineering*. Newnes, 2012, ISBN: 978-0-08-096912-1.

[17] N. D. Lian, 'Modellering av dimensjonerende elspesifikk last for leiligheter i fjellhamar bruk,' 2018.

[18] T. Wildi, *Electrical Machines, Drives, and Power Systems*. Pearson Education Limited, 2014, ISBN: 978-1-292-02458-5.

[19] J. D. Whiteside, *Calculating wire temperature is not complicated (nichrome example)*, 2018. [Online]. Available: https://www.youtube.com/watch?v=QNSOLrlRHbs&t=1671s (visited on 14/05/2022).

[20] REN AS, 'Samhandling mellom nettselskap og kunde ved tilknytning,' 4102, 2021.

[21] REN AS, 'Teknisk/økonomisk vurdering av forsyning til grisgrendte strøk i ls-nett,' 8072, 2020.

[22] V. E. Minas Patsalides Andreas Stavrou and G. E. Georghiou, 'Assessing the level of harmonic distortion due to pv generation in mini grids,' 2014.

[23] C. B. Honsberg and S. G. Bowden. 'Photovoltaics eduction website.' (2019), [Online]. Available: www.pveducation.org (visited on 13/05/2022).

[24] Photon, *Photon inverter tests*, https://www.photon.info/en/inverter-tests, Accessed: 30.04.2022.

[25] D. S. Phillips and W. Warmuth, 'Photovoltaics report,' 2022.

[26] PVsyst. 'Performance ratio pr.' (), [Online]. Available: https://www.pvsyst.com/help/performance_ratio.htm (visited on 10/05/2022).

[27] NVE-RME. 'Quality of electricity supply.' (2021), [Online]. Available: https://2021.nve.no/norwegian-energy-regulatory-authority/network-regulation/quality-of-electricity-supply/ (visited on 13/05/2022).

[28] E. Vaahedi, *Practical Power System Operation*. John Wiley @ Sons, Inc, 2013, ISBN: 978-1-118-39402-1.

[29] C. Seneviratne and C. R. Ozansoy, 'Frequency response due to a large generator loss with the increasing penetration of wind/pv generation - a literature review,' 57, 2016.

[30] H. K. et al., 'Veiledere for utfordrende elektriske apparater,' 386, 2015.

[31] REN AS, ‘Råd om nettanalyse ved kraftproduksjon,’ 3006, 2020.

[32] REN AS, ‘Tekniske funksjonskrav til tilknytnings. og nettleieavtale for innmatingskunder i lavspenningsnettet,’ 347, 2020.

[33] S. M. Ahsan, H. A. Khan, A. Hussain, S. Tariq and N. A. Zaffar, ‘Harmonic analysis of grid-connected solar pv systems with nonlinear household loads in low-voltage distribution networks,’ no. 3709, 2021, `https://www.researchgate.net/publication/350459033_Harmonic_Analysis_of_Grid-Connected_Solar_PV_Systems_with_Nonlinear_Household_Loads_in_Low-Voltage_Distribution_Networks`.

[34] M. B. Marz, ‘Interharmonics: What they are, where they come from and what they do,’ 2016.

[35] V. Ravindran, S. K. Rönnberg, T. Busatto and M. H. J. Bollen, ‘Inspection of interharmonic emissions from a grid-tied pv inverter in north sweden,’ *2018 18th International Conference on Harmonics and Quality of Power (ICHQP)*, pp. 1–6, 2018.

[36] A. Haddad and D. Warne, *Advances in High Voltage Engineering.* IET Power and energy series 40, 2009, ISBN: 978-1-84919-038-1.

[37] Y. Zhang, H. Chen and Y. P. Du, ‘Transients in solar photovoltaic systems during lightning strikes to a transmission line,’ *International Journal of Electrical Power and Energy Systems*, vol. 134, Jan. 2022. DOI: `10.1016/j.ijepes.2021.106885`.

[38] Jaymala D. Pradhan, Somnath S. Hadpe and Rakesh G. Shriwastava, ‘Analysis and design of overcurrent protection for grid-connected microgrid with pv generation,’ Apr. 2022. DOI: `https://doi.org/10.1016/j.gltp.2022.03.023`.

[39] L. Namangolwa and E. Begumisa, ‘Impacts of solar photovoltaic on the protection system of distribution networks,’ Chalmars University of Technology, 2016.

[40] DIgSILENT GmbH. ‘Power system software and engineering.’ (), [Online]. Available: `https://www.digsilent.de/en/` (visited on 08/05/2022).

[41] Trimble Inc. ‘Trimble nis for electric utilities.’ (), [Online]. Available: `https://upa.trimble.com/en/products/trimble-nis-electric` (visited on 08/05/2022).

[42] DIgSILENT GmbH. ‘Power quality and harmonic analysis.’ (), [Online]. Available: `https://www.digsilent.de/en/power-quality-and-harmonic-analysis.html` (visited on 08/05/2022).

[43] D. J. Pannell, ‘Sensitivity analysis of normative economic models: Theoretical framework and practical strategies,’ 16, 1996.

[44] REN AS, ‘Kraftproduksjon - tiltak for økt tilknytningskapasitet,’ 3010, 2020.

[45] A. van Dijk Festøy, ‘Voltage regulation in low voltage distribution grids,’ Norwegian University of Science and Technology, Jun. 2020.

[46] R. Tjeldhorn and L. Røssland, 'Spenningsregulering i distribusjonsnettet,' 2017.

[47] A. Petterteig. 'Smart aktiv regulering av spenning og reaktiv effekt i nett med lokal produksjon.' (2011), [Online]. Available: `http://www.energy.sintef.no/Prosjekt/Distribution_2020` (visited on 26/03/2022).

[48] Y. Wang, K. T. Tan, X. Y. Peng and P. L. So, 'Coordinated control of distributed energy-storage systems for voltage regulation in distribution networks,' 3, 2016.

[49] M. Melkevik, 'Avoiding voltage rise in distribution grids using energy storage systems,' Norwegian University of Science and Technology, Aug. 2016.

[50] Lede AS. 'Som plusskunde kan du produsere og selge din egen strøm.' (), [Online]. Available: `https://lede.no/plusskunde/category2788.html` (visited on 16/05/2022).

[51] Transformers Committee of the IEEE Power and Energy Society, 'Ieee standard test code for liquid-immersed distribution, power, and regulating transformers,' C57.12.90-2015, 2015.

# Appendix A

# Project description

University of South-Eastern Norway

**Faculty of Technology, Natural Sciences and Maritime Sciences, Campus Porsgrunn**

# FM4017 Project

**<u>Title</u>**: Criteria for grid investments to satisfy customer requirements under higher PV-system penetration from households.

**<u>USN supervisor</u>**: Thomas Øyvang and Gunne J. Hegglid

**<u>External partner</u>**: Lede AS – Marte Neslow

**<u>Task background</u>**:
In the past decade, there has been increasing growth in PV systems. These systems are integrated into the customers of the DSO, being able to cause more unreliable consumption/production and therefore also problems for voltage quality. Lede AS wants to investigate the development of PV installations and how to make the correct investment to ensure voltage quality according to the requirements of Norwegian regulations. Today when a customer connects to the grid, they are granted a level of current/power to consume electricity from the grid. According to today's regulations, the customer is entitled to produce the same level of current back into the grid.

**<u>Task description</u>**:
The student should consider the following parts:
The main objective of this thesis is to find the threshold/index for when new PV installations in households causes a necessity to invest in the grid because of voltage quality

- Find a threshold that can be used to determine when the grid needs investment to handle new PV installation for households in the grid.
  - Using existing reports and if necessary perform own calculations to find which parameters affect the voltage quality of the grid
  - Consider the use of an analysis tool and/or study case to support the thesis. Quantitative analyses are of interest.
  - Consider the Norwegian quality regulations for delivering electricity for different parameters that could cause a necessity of investment (e.g., asymmetric voltage, rapid and slow voltage change, THD and over harmonic current and short circuit currents). Moreover, do field measurements with Medcal instrument if needed for a better basis for the conclusions (noise etc).
- Map the development of PV-installations
  - Find and evaluate the parameters to describe development—for instance, the number of installations per year and size of installations.
- Investigate the future need for measures in the grid to meet the growth of PV-installations
  - Map the low voltage grid-circuits of Lede AS with a focus on parameters that affects voltage quality
  - Use obtained data to predict the development of needed measures to meet PV-installation growth.
- Investigate different measures that can be used
  - Traditional grid investment with upscaling transformer, cables and lines.

- Smart grid components (Auto-tap-changer, AVR, reactive component in grid)
- Flexible customers by agreements of production and/or load control

**Student category**: EPE

**The task is suitable for students not present at the campus (e.g. online students)**: Yes

**Practical arrangements**:
Calculations using Network Information System (NIS) with data from DSO. If necessary, USN or Lede will provide other relevant analysis tools during thesis work.

**Signatures**:

Supervisor (date and signature):

01/02/2022 Thomas Øyvang 1/2-22

Student (write clearly in all capitalized letters + date and signature):

ANDERS BERGER Anders Berger 1/2-22

**Signatur:** Thomas Øyvang 1/2-22
Thomas Øyvang 1/2-22 (1. Feb. 2022 17:18 GMT+1)

**E-post:** thomas.oyvang@usn.no

# Appendix B

# PowerFactory circuits

# Circuit 1

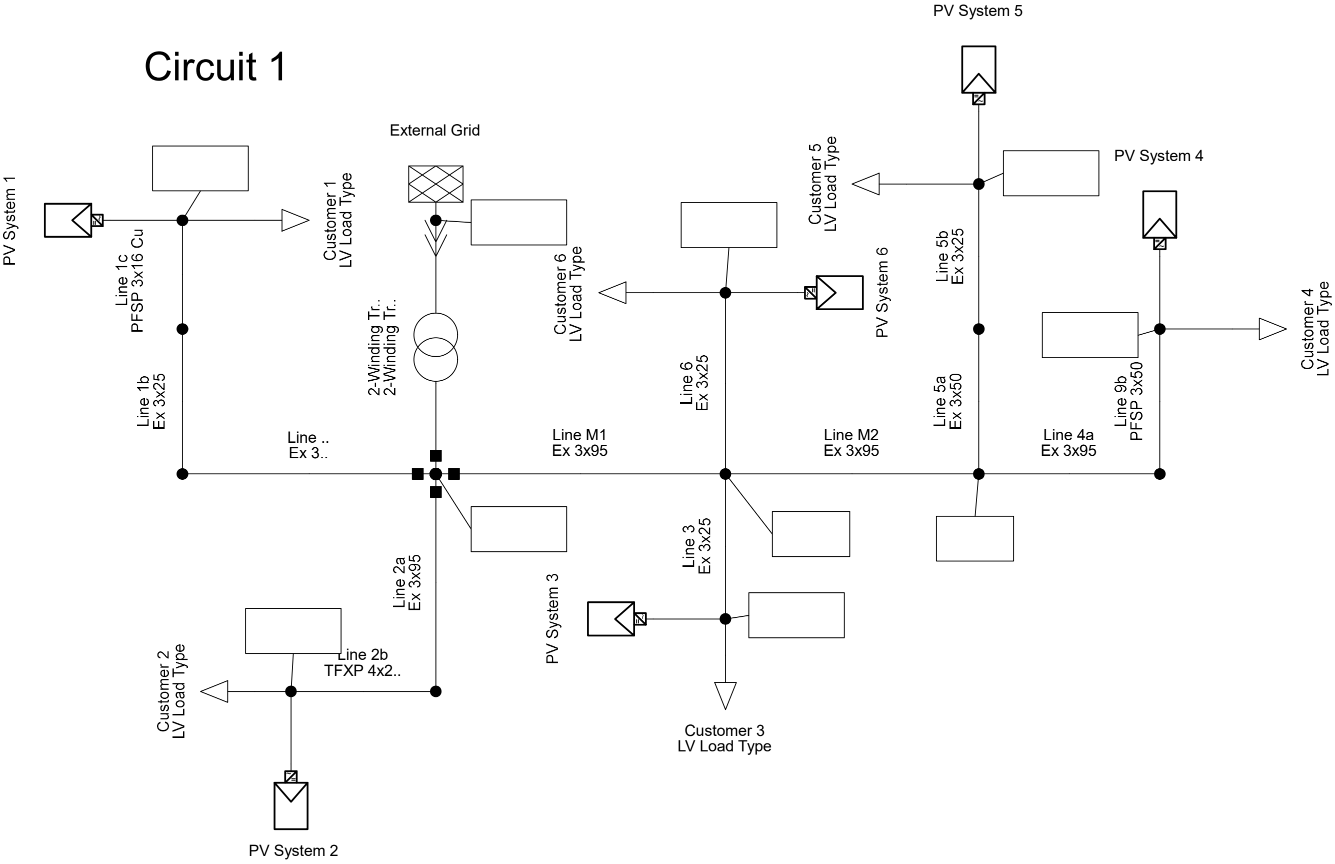

PV System 5
External Grid
PV System 4
Customer 5
LV Load Type
PV System 1
Customer 1
LV Load Type
Line 1c
PFSP 3x16 Cu
Customer 6
LV Load Type
PV System 6
Line 5b
Ex 3x25
Customer 4
LV Load Type
2-Winding Tr..
2-Winding Tr..
Line 1b
Ex 3x25
Line 6
Ex 3x25
Line 5a
Ex 3x50
Line 9b
PFSP 3x50
Line ..
Ex 3..
Line M1
Ex 3x95
Line M2
Ex 3x95
Line 4a
Ex 3x95
Line 3
Ex 3x25
Line 2a
Ex 3x95
PV System 3
Line 2b
TFXP 4x2..
Customer 2
LV Load Type
Customer 3
LV Load Type
PV System 2

# Circuit 2

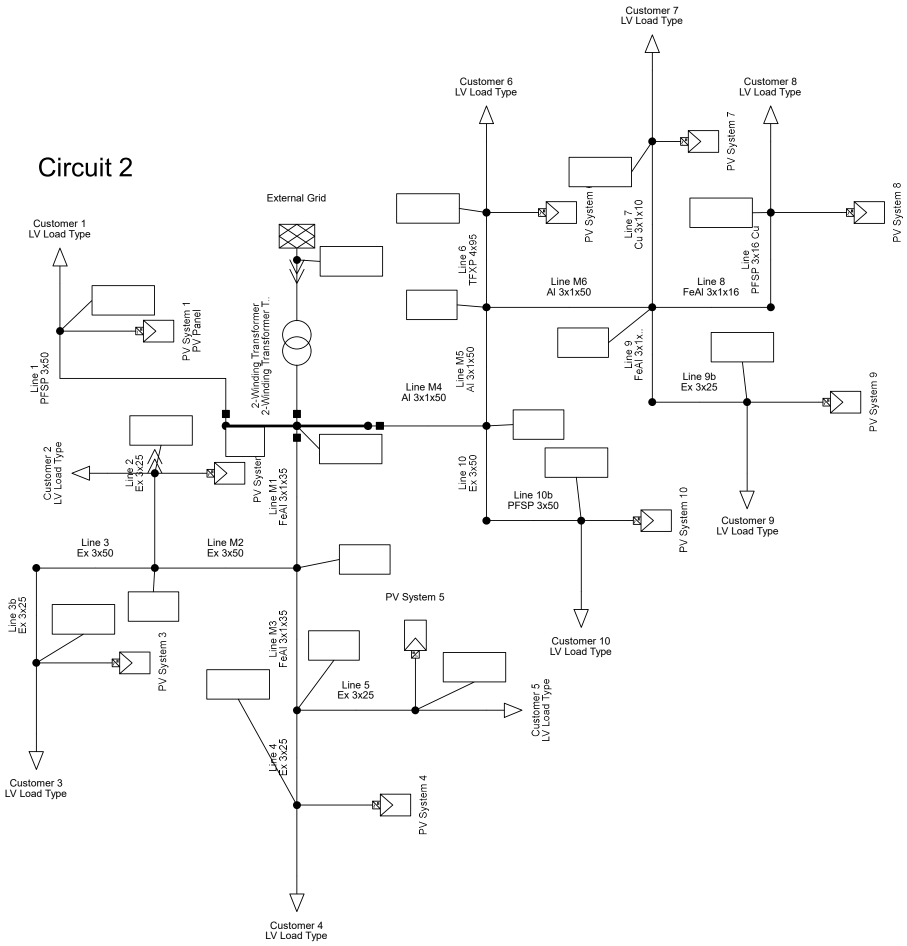
External Grid
2-Winding Transformer
2-Winding Transformer T..
Customer 1
LV Load Type
PV System 1
PV Panel
Line 1
PFSP 3x50
Customer 2
LV Load Type
Line 2
Ex 3x25
PV System
Line M1
FeAl 3x1x35
Line 3
Ex 3x50
Line M2
Ex 3x50
Line 3b
Ex 3x25
PV System 3
Customer 3
LV Load Type
Line M3
FeAl 3x1x35
PV System 5
Line 5
Ex 3x25
Customer 5
LV Load Type
Line 4
Ex 3x25
PV System 4
Customer 4
LV Load Type
Line M4
Al 3x1x50
Line M5
Al 3x1x50
Line 6
TFXP 4x95
Customer 6
LV Load Type
PV System
Line M6
Al 3x1x50
Customer 7
LV Load Type
PV System 7
Line 7
Cu 3x1x10
Customer 8
LV Load Type
PV System 8
Line
PFSP 3x16 Cu
Line 8
FeAl 3x1x16
Line 9
FeAl 3x1x..
Line 9b
Ex 3x25
PV System 9
Customer 9
LV Load Type
Line 10
Ex 3x50
Line 10b
PFSP 3x50
PV System 10
Customer 10
LV Load Type

# Circuit 3

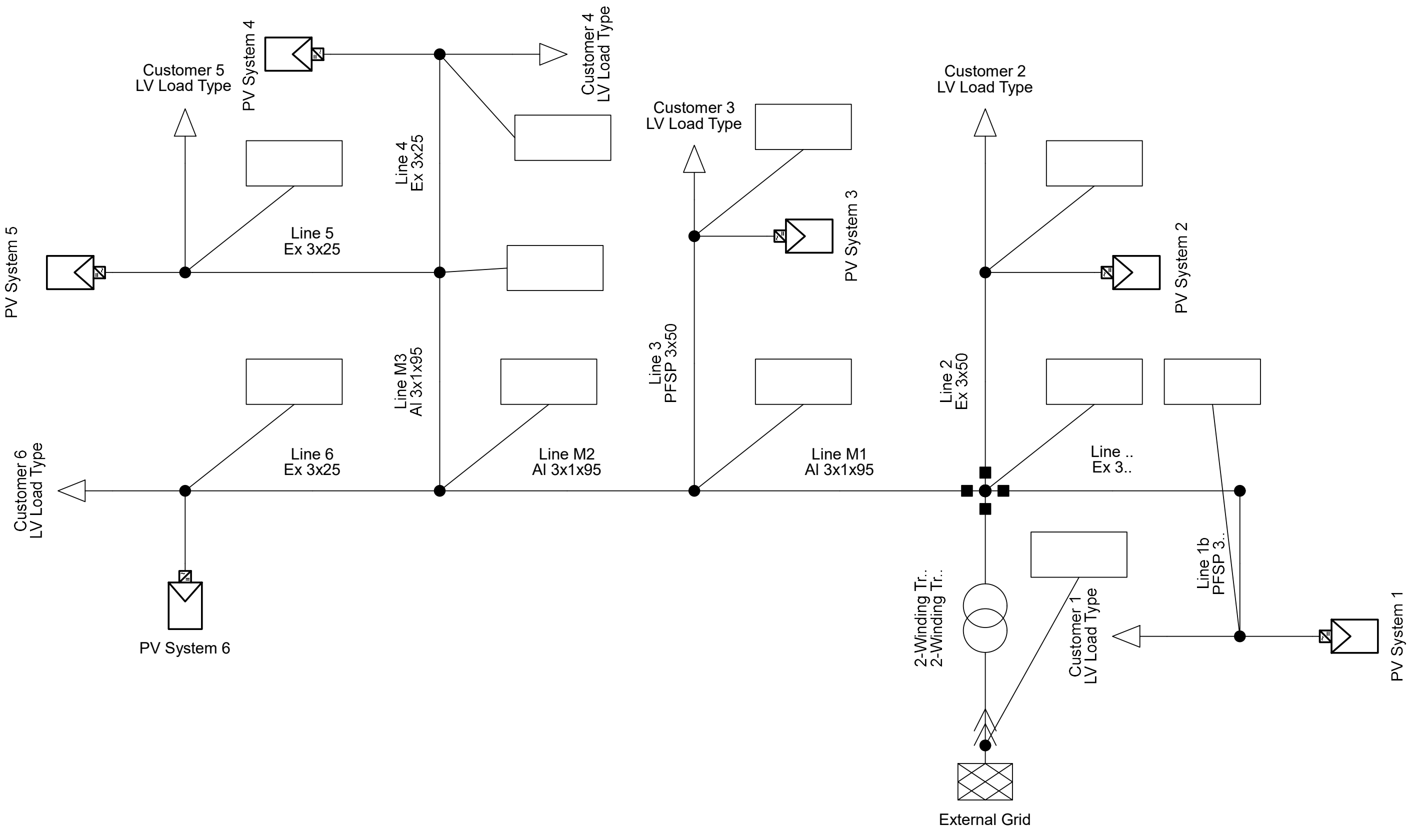

PV System 4
Customer 4
LV Load Type
Customer 5
LV Load Type
Customer 3
LV Load Type
Customer 2
LV Load Type
Line 4
Ex 3x25
Line 5
Ex 3x25
PV System 5
PV System 3
PV System 2
Line M3
Al 3x1x95
Line 3
PFSP 3x50
Line 2
Ex 3x50
Line 6
Ex 3x25
Line M2
Al 3x1x95
Line M1
Al 3x1x95
Line ..
Ex 3..
Customer 6
LV Load Type
Line 1b
PFSP 3..
2-Winding Tr..
2-Winding Tr..
Customer 1
LV Load Type
PV System 6
PV System 1
External Grid

# Circuit 4

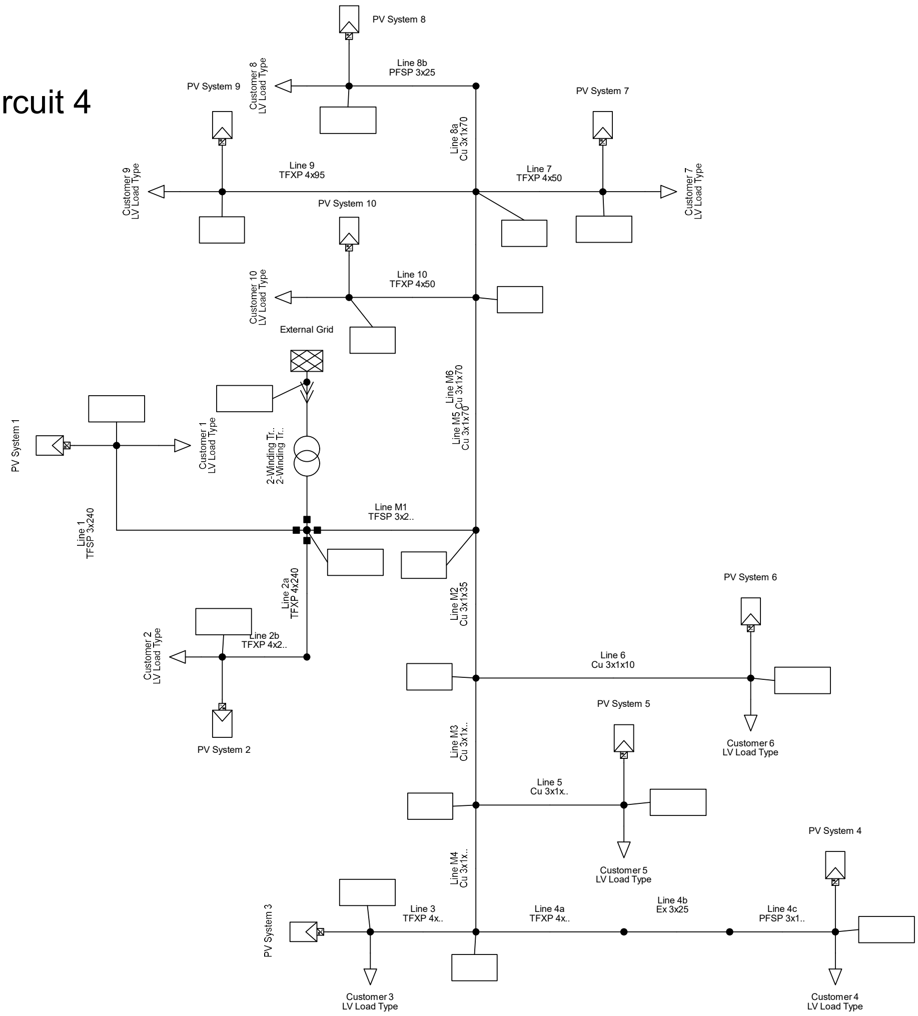

PV System 8
Line 8b
PFSP 3x25
Customer 8
LV Load Type
PV System 9
PV System 7
Line 8a
Cu 3x1x70
Line 9
TFXP 4x95
Line 7
TFXP 4x50
Customer 9
LV Load Type
Customer 7
LV Load Type
PV System 10
Line 10
TFXP 4x50
Customer 10
LV Load Type
External Grid
Line M6
Line M5 Cu 3x1x70
Cu 3x1x70
PV System 1
Customer 1
LV Load Type
2-Winding Tr..
2-Winding Tr..
Line M1
TFSP 3x2..
Line 1
TFSP 3x240
Line 2a
TFXP 4x240
Line M2
Cu 3x1x35
PV System 6
Customer 2
LV Load Type
Line 2b
TFXP 4x2..
Line 6
Cu 3x1x10
PV System 2
PV System 5
Customer 6
LV Load Type
Line M3
Cu 3x1x..
Line 5
Cu 3x1x..
Customer 5
LV Load Type
PV System 4
Line M4
Cu 3x1x..
Line 3
TFXP 4x..
Line 4a
TFXP 4x..
Line 4b
Ex 3x25
Line 4c
PFSP 3x1..
PV System 3
Customer 3
LV Load Type
Customer 4
LV Load Type

# Appendix C

# Data used in PowerFactory

## External grid data

| Circuit 1 | | |
|---|---|---|
| Active power | 20 | MW |
| Reactive power | 10 | Mvar |
| Voltage Setpoint | 1,018 | pu |
| **Max values** | | |
| Short-Circuit Current Ik''max | 4,489 | kA |
| c-factor (max) | 1,1 | |
| R/X Ratio | 0,04795 | |
| **Min values** | | |
| Short-Circuit Current Ik''min | 1,12 | kA |
| c-factor (max) | 0,9 | |
| R/X Ratio | 0,04795 | |

| Circuit 2 | | |
|---|---|---|
| Active power | 20 | MW |
| Reactive power | 10 | Mvar |
| Voltage Setpoint | 0,995 | pu |
| **Max values** | | |
| Short-Circuit Current Ik''max | 3,58 | kA |
| c-factor (max) | 1,1 | |
| R/X Ratio | 0,04795 | |
| **Min values** | | |
| Short-Circuit Current Ik''min | 0,805 | kA |
| c-factor (max) | 0,9 | |
| R/X Ratio | 0,04795 | |

| Circuit 3 | | |
|---|---|---|
| Active power | 20 | MW |
| Reactive power | 10 | Mvar |
| Voltage Setpoint | 0,921 | pu |
| **Max values** | | |
| Short-Circuit Current Ik''max | 5,852 | kA |
| c-factor (max) | 1,1 | |
| R/X Ratio | 0,04508 | |
| **Min values** | | |
| Short-Circuit Current Ik''min | 0,8745 | kA |
| c-factor (max) | 0,9 | |
| R/X Ratio | 0,04508 | |

| Circuit 4 | | |
|---|---|---|
| Active power | 20 | MW |
| Reactive power | 10 | Mvar |
| Voltage Setpoint | 1,018 | pu |
| **Max values** | | |
| Short-Circuit Current Ik''max | 4,115 | kA |
| c-factor (max) | 1,1 | |
| R/X Ratio | 0,0336 | |
| **Min values** | | |
| Short-Circuit Current Ik''min | 2,082 | kA |
| c-factor (max) | 0,9 | |
| R/X Ratio | 0,0336 | |

# Transformer data

| Circuit 1 | | |
|---|---|---|
| Rated power | 100 | kVA |
| Rated Voltage primary | 22 | kV |
| Rated Voltage secondary | 0,24 | kV |
| | | |
| Short-Circuit Voltage uk impedance | 4 | % |
| Copper losses | 1,566 | kW |
| Short-Circuit Voltage uk resistance | 1,56 | % |
| No Load losses | 0,289 | kW |
| | | |
| Tap Changer | 2,5 | % |
| Positions | 5 | |

| Circuit 2 | | |
|---|---|---|
| Rated power | 100 | kVA |
| Rated Voltage primary | 22 | kV |
| Rated Voltage secondary | 0,24 | kV |
| | | |
| Short-Circuit Voltage uk impedance | 4,15 | % |
| Copper losses | 1,615 | kW |
| Short-Circuit Voltage uk resistance | 1,615 | % |
| No Load losses | 0,247 | kW |
| | | |
| Tap Changer | 2,5 | % |
| Positions | 5 | |

| Circuit 3 | | |
|---|---|---|
| Rated power | 50 | kVA |
| Rated Voltage primary | 22 | kV |
| Rated Voltage secondary | 0,24 | kV |
| | | |
| Short-Circuit Voltage uk impedance | 3,94 | % |
| Copper losses | 1,068 | kW |
| Short-Circuit Voltage uk resistance | 3,94 | % |
| No Load losses | 0,164 | kW |
| | | |
| Tap Changer | 2,5 | % |
| Positions | 7 | |

| Circuit 4 | | |
|---|---|---|
| Rated power | 315 | kVA |
| Rated Voltage primary | 22 | kV |
| Rated Voltage secondary | 0,24 | kV |
| | | |
| Short-Circuit Voltage uk impedance | 4,61 | % |
| Copper losses | 3,003 | kW |
| Short-Circuit Voltage uk resistance | 0,953 | % |
| No Load losses | 0,66 | kW |
| | | |
| Tap Changer | 2,5 | % |
| Positions | 5 | |

**200 kVA - Used in changing transformer case**

| | | |
|---|---|---|
| Rated power | 200 | kVA |
| Rated Voltage primary | 22 | kV |
| Rated Voltage secondary | 0,24 | kV |
| | | |
| Short-Circuit Voltage uk impedance | 4,4 | % |
| Copper losses | 2,016 | kW |
| Short-Circuit Voltage uk resistance | 1,008 | % |
| No Load losses | 0,583 | kW |
| | | |
| Tap Changer | 2,5 | % |
| Positions | 5 | |

**500 kVA - Used in changing transformer case**

| | | |
|---|---|---|
| Rated power | 500 | kVA |
| Rated Voltage primary | 22 | kV |
| Rated Voltage secondary | 0,24 | kV |
| | | |
| Short-Circuit Voltage uk impedance | 4,68 | % |
| Copper losses | 5,529 | kW |
| Short-Circuit Voltage uk resistance | 1,106 | % |
| No Load losses | 0,469 | kW |
| | | |
| Tap Changer | 2,5 | % |
| Positions | 7 | |

# Datasheet for cables and lines

| Type | Rated current [A] | R [Ohm/km] | X [Ohm/km] | R0 [Ohm/km] | X0 [Ohm/km] |
|---|---|---|---|---|---|
| Al 3x1x95 | 385 | 0,19 | 0,215 | 0,19 | 0 |
| Al 3x1x70 | 305 | 0,257 | 0,225 | 0,257 | 0 |
| Al 3x1x25 | 158 | 0,718 | 0,257 | 0,718 | 0 |
| AL 3x1x16 | 120 | 1,123 | 0,271 | 1,123 | 0 |
| Cu 3x1x70 | 282 | 0,259 | 0,24 | 0,259 | 0 |
| Cu 3x1x35 | 174 | 0,515 | 0,261 | 0,515 | 0 |
| Cu 3x1x16 | 115 | 1,113 | 0,294 | 1,113 | 0 |
| Cu 3x1x10 | 80 | 1,178 | 0,294 | 1,113 | 0 |
| Ex 3x95 Al | 280 | 0,308 | 0,075 | 0,32 | 0 |
| Ex 3x50 AL | 180 | 1,178 | 0,079 | 0,32 | 0 |
| Ex 3x25 Al | 115 | 1,2 | 0,082 | 1,2 | 0 |
| FeAl 3x70 | 468 | 0,258 | 0,22 | 0,258 | 0 |
| FeAl 3x50 | 352 | 0,361 | 0,231 | 0,361 | 0 |
| FeAl 3x35 | 284 | 0,515 | 0,252 | 0,515 | 0 |
| FeAl 3x16 | 180 | 1,131 | 0,267 | 1,131 | 0 |
| PFSP 3x240 AL | 375 | 0,125 | 0,072 | 0,125 | 0 |
| PFSP 3x95 Al | 220 | 0,32 | 0,075 | 0,253 | 0 |
| PFSP 3x50 Al | 150 | 0,641 | 0,079 | 0,641 | 0 |
| PFSP 3x25 AL | 100 | 1,2 | 0,082 | 1,2 | 0 |
| PFSP 3x16 Cu | 100 | 1,15 | 0,085 | 0,727 | 0 |
| TFSP 3x240 Al | 435 | 0,125 | 0,081 | 0,125 | 0 |
| TFXP 4x240 Al | 435 | 0,125 | 0,081 | 0,125 | 0,39 |
| TFXP 4x95 Al | 260 | 0,32 | 0,082 | 0,32 | 0,24 |
| TFXP 4x50 Al | 180 | 0,641 | 0,086 | 0,641 | 0,32 |
| TFXP 4x25 Al | 125 | 1,2 | 0,086 | 1,2 | 0,3 |

# Overview of cables and lines

**Circuit 1**

| Line | Node 1 | Node 2 | Length [m] | Type |
|---|---|---|---|---|
| Line M1 | Bus substation | Bus M1 | 215 | Ex 3x95 Al |
| Line M2 | Bus M1 | Bus M2 | 62 | Ex 3x95 Al |
| Line 1a | Bus substation | Bus 1a | 62 | Ex 3x95 Al |
| Line 1b | Bus 1a | Bus 1b | 142 | Ex 3x25 Al |
| Line 1c | Bus 1b | Bus 1c | 24 | PFSP 3x16 Cu |
| Line 2a | Bus substation | Bus 2a | 117 | Ex 3x95 Al |
| Line 2b | Bus 2a | Bus 2b | 196 | TFXP 4x240 Al |
| Line 3 | Bus M2 | Bus 3 | 72 | Ex 3x25 Al |
| Line 4a | Bus M2 | Bus 4a | 286 | Ex 3x95 Al |
| Line 4b | Bus 4a | Bus 4b | 11 | PFSP 3x50 Al |
| Line 5a | Bus M2 | Bus 5a | 61 | Ex 3x50 Al |
| Line 5b | Bus 5a | Bus 5b | 286 | Ex 3x25 Al |
| Line 6 | Bus M1 | Bus 6a | 25 | Ex 3x25 Al |

**Circuit 2**

| Line | Node 1 | Node 2 | Length [m] | Type |
|---|---|---|---|---|
| Line M1 | Bus substation | Bus M1 | 310 | FeAl 3x1x35 |
| Line M2 | Bus M1 | Bus M2 | 32 | Ex 3x50 Al |
| Line M3 | Bus M1 | Bus M3 | 189 | FeAl 3x1x35 |
| Line M4 | Bus substation | Bus M4 | 25 | Al 3x1x50 |
| Line M5 | Bus M4 | Bus M5 | 34 | Al 3x1x50 |
| Line M6 | Bus M5 | Bus M6 | 115 | FeAl 3x1x35 |
| Line 1 | Bus substation | Bus 1 | 83 | PFSP 3x50 |
| Line 2 | Bus M2 | Bus 2 | 22 | Ex 3x25 Al |
| Line 3a | Bus M2 | Bus 3a | | Ex 3x50 Al |
| Line 3b | Bus 3a | Bus 3b | 38 | Ex 3x25 Al |
| Line 4 | Bus M3 | Bus 4 | 18 | Ex 3x25 Al |
| Line 5 | Bus M3 | Bus 5 | 10 | Ex 3x25 Al |
| Line 6 | Bus M5 | Bus 6 | 65 | TFXP 4x95 Al |
| Line 7 | Bus M6 | Bus 7 | 35 | Cu 3x1x10 |
| Line 8 | Bus M6 | Bus 8 | 80 | FeAl 3x1x35 |
| Line 9a | Bus M6 | Bus 9a | 50 | FeaAl 3x1x16 |
| Line 9b | Bus 9a | Bus 9b | 29 | Ex 3x25 Al |
| Line 10a | Bus M4 | Bus 10a | 40 | Ex 3x50 Al |
| Line 10b | Bus 10a | Bus 10b | 33 | PFSP 3x50 Al |

**Circuit 3**

| Line | Node 1 | Node 2 | Length [m] | Type |
|---|---|---|---|---|
| Line M1 | Bus substation | Bus M1 | 63,4 | Al 3x1x95 |
| Line M2 | Bus M1 | Bus M2 | 196 | Al 3x1x95 |
| Line M3 | Bus M2 | Bus M3 | 117,8 | Al 3x1x95 |
| Line 1a | Bus substation | Bus 1a | 75 | Ex 3x95 Al |
| Line 1b | Bus 1a | Bus 1b | 14,9 | PFSP 3x95 Al |
| Line 2 | Bus substation | Bus 2 | 88,2 | Ex 3x50 Al |
| Line 3 | Bus M1 | Bus 3 | 29,3 | PFSP 3x50 Al |
| Line 4 | Bus M3 | Bus 4 | 14,9 | Ex 3x25 Al |
| Line 5 | Bus M3 | Bus 5 | 55,8 | Ex 3x25 Al |
| Line 6 | Bus M2 | Bus 6 | 9,2 | Ex 3x25 Al |

**Circuit 4**

| Line | Node 1 | Node 2 | Length [m] | Type |
|---|---|---|---|---|
| Line M1 | Bus substation | Bus M1 | 21,9 | TFSP 3x240 Al |
| Line M2 | Bus M1 | Bus M2 | 29,1 | Cu 3x1x35 |
| Line M3 | Bus M1 | Bus M3 | 42,5 | Cu 3x1x35 |
| Line M4 | Bus substation | Bus M4 | 48,1 | Cu 3x1x16 |
| Line M5 | Bus M4 | Bus M5 | 39,7 | Cu 3x1x70 |
| Line M6 | Bus M5 | Bus M6 | 111,3 | Cu 3x1x70 |
| Line 1 | Bus substation | Bus 1 | 25,7 | TFSP 2x3x240 AL |
| Line 2a | Bus substation | Bus 2a | 584,5 | TFXP 4x240 Al |
| Line 2b | Bus 2a | Bus 2b | 4 | TFXP 4x240 Al |
| Line 3 | Bus M4 | Bus 3 | 42,1 | TFXP 4x50 Al |
| Line 4a | Bus M4 | Bus 4a | 88,8 | TFXP 4x50 Al |
| Line 4b | Bus 4a | Bus 4b | 80,1 | Ex 3x25 Al |
| Line 4c | Bus 4b | Bus 4c | 42,5 | PFSP 3x16 Cu |
| Line 5 | Bus M3 | Bus 5 | 12,9 | Cu 3x1x10 |
| Line 6 | Bus M2 | Bus 6 | 15,4 | Cu 3x1x10 |
| Line 7 | Bus M6 | Bus 7 | 5,9 | TFXP 4x50 Al |
| Line 8a | Bus M6 | Bus 8a | 144,6 | Cu 3x1x70 |
| Line 8b | Bus 8a | Bus 8b | 65,6 | PFSP 3x25 Al |
| Line 9 | Bus M6 | Bus 9 | 1,5 | PFSP 3x95 Al |
| Line 10 | Bus M5 | Bus 10 | 19,6 | TFXP 4x50 Al |

## Winter load and summer load

**Circuit 1**

| Customer | Winter load [kWh/h] | Summer load [kWh/h] |
|---|---|---|
| Customer 1 | 8,965 | 1,977 |
| Customer 2 | 37,800 | 20,000 |
| Customer 3 | 19,603 | 6,276 |
| Customer 4 | 10,060 | 3,896 |
| Customer 5 | 4,493 | 0,791 |
| Customer 6 | 9,588 | 1,878 |

**Circuit 2**

| Customer | Winter load [kWh/h] | Summer load [kWh/h] |
|---|---|---|
| Customer 1 | 16,320 | 4,693 |
| Customer 2 | 2,475 | 0,346 |
| Customer 3 | 8,593 | 1,360 |
| Customer 4 | 4,930 | 1,773 |
| Customer 5 | 8,626 | 2,338 |
| Customer 6 | 7,646 | 0,366 |
| Customer 7 | 10,781 | 0,681 |
| Customer 8 | 7,725 | 0,901 |
| Customer 9 | 7,506 | 1,279 |
| Customer 10 | 12,575 | 2,253 |

**Circuit 3**

| Customer | Winter load [kWh/h] | Summer load [kWh/h] |
|---|---|---|
| Customer 1 | 11,465 | 2,053 |
| Customer 2 | 6,147 | 2,300 |
| Customer 3 | 5,941 | 0,803 |
| Customer 4 | 8,757 | 3,866 |
| Customer 5 | 6,351 | 2,320 |
| Customer 6 | 6,941 | 9,916 |

**Circuit 4**

| Customer | Winter load [kWh/h] | Summer load [kWh/h] |
|---|---|---|
| Customer 1 | 38,587 | 0,400 |
| Customer 2 | 19,600 | 6,500 |
| Customer 3 | 8,739 | 1,520 |
| Customer 4 | 6,358 | 1,192 |
| Customer 5 | 8,934 | 2,102 |
| Customer 6 | 4,001 | 0,050 |
| Customer 7 | 2,649 | 0,000 |
| Customer 8 | 11,737 | 1,875 |
| Customer 9 | 22,374 | 3,967 |
| Customer 10 | 20,592 | 2,652 |

# Appendix D

# Short circuit calculations

# Short circuit calculations in Trimble and PowerFactory

**Circuit 1**

| | Trimble | | PowerFactory | | 200 kVA | | Feeding lines | |
|---|---|---|---|---|---|---|---|---|
| | Isc2min | Isc3max | Isc2min | Isc3max | Isc2min | Isc3max | Isc2min | Isc3max |
| Customer 1 | 387 | 605 | 387 | 606 | 397 | 626 | 387 | 606 |
| Customer 2 | 1185 | 1738 | 1115 | 2655 | 1234 | 1869 | 1115 | 1655 |
| Customer 3 | 536 | 811 | 529 | 822 | 550 | 862 | 698 | 1073 |
| Customer 4 | 450 | 678 | 438 | 677 | 452 | 705 | 545 | 834 |
| Customer 5 | 196 | 306 | 184 | 289 | 186 | 293 | 201 | 316 |
| Customer 6 | 762 | 1120 | 793 | 1217 | 844 | 1314 | 1214 | 1807 |

**Circuit 2**

| | Trimble | | PowerFactory | | 200 kVA | | Feeding lines | |
|---|---|---|---|---|---|---|---|---|
| | Isc2min | Isc3max | Isc2min | Isc3max | Isc2min | Isc3max | Isc2min | Isc3max |
| Customer 1 | 1409 | 2103 | 1346 | 2032 | 1518 | 2357 | 1346 | 2036 |
| Customer 2 | 405 | 616 | 384 | 585 | 397 | 610 | 859 | 1294 |
| Customer 3 | 372 | 568 | 354 | 542 | 365 | 563 | 726 | 1103 |
| Customer 4 | 274 | 419 | 262 | 400 | 268 | 411 | 421 | 640 |
| Customer 5 | 309 | 468 | 293 | 445 | 301 | 460 | 507 | 762 |
| Customer 6 | 1458 | 2098 | 1456 | 2121 | 1697 | 2538 | 1960 | 2839 |
| Customer 7 | 730 | 1078 | 695 | 1033 | 742 | 1119 | 792 | 1179 |
| Customer 8 | 465 | 709 | 467 | 711 | 486 | 748 | 509 | 777 |
| Customer 9 | 538 | 538 | 506 | 769 | 529 | 813 | 556 | 847 |
| Customer 10 | 1232 | 1232 | 1268 | 1905 | 1426 | 2200 | 1402 | 2111 |

**Circuit 3**

| | Trimble | | PowerFactory | | 100 kVA | | Feeding lines | |
|---|---|---|---|---|---|---|---|---|
| Customer | Isc2min | Isc3max | Isc2min | Isc3max | Isc2min | Isc3max | Isc2min | Isc3max |
| Customer 1 | 1439 | 1989 | 1430 | 2020 | 2003 | 2940 | 1430 | 2020 |
| Customer 2 | 1083 | 1559 | 1033 | 1514 | 1281 | 1946 | 1033 | 1514 |
| Customer 3 | 1268 | 1751 | 1297 | 1818 | 1760 | 2539 | 1461 | 2054 |
| Customer 4 | 746 | 1036 | 704 | 993 | 821 | 1175 | 794 | 1126 |
| Customer 5 | 559 | 810 | 530 | 775 | 591 | 879 | 575 | 847 |
| Customer 6 | 1038 | 1419 | 983 | 1372 | 1229 | 1746 | 1171 | 1643 |

**Circuit 4**

| | Trimble | | PowerFactory | | 500 kVA | | Feeding lines | |
|---|---|---|---|---|---|---|---|---|
| | Isc2min | Isc3max | Isc2min | Isc3max | Isc2min | Isc3max | Isc2min | Isc3max |
| Customer 1 | 10887 | 14079 | 10214 | 13917 | 14116 | 19558 | 10214 | 13917 |
| Customer 2 | 1048 | 1546 | 1003 | 1485 | 1022 | 1519 | 1003 | 1485 |
| Customer 3 | 686 | 1059 | 692 | 1069 | 698 | 1081 | 764 | 1182 |
| Customer 4 | 290 | 455 | 293 | 460 | 294 | 462 | 305 | 479 |
| Customer 5 | 1481 | 2223 | 1413 | 2133 | 1444 | 2194 | 1751 | 2634 |
| Customer 6 | 2171 | 3244 | 2114 | 3183 | 2186 | 3322 | 2970 | 4439 |
| Customer 7 | 1441 | 2074 | 1452 | 2092 | 1497 | 2168 | 1652 | 2386 |
| Customer 8 | 497 | 756 | 506 | 768 | 510 | 775 | 527 | 801 |
| Customer 9 | 1425 | 2051 | 1520 | 2176 | 1571 | 2261 | 1741 | 2497 |
| Customer 10 | 2372 | 3517 | 2728 | 4020 | 2869 | 4280 | 3511 | 5231 |